"Mimetic Finite-Difference Method
for
Diffusion Equations
on
Polyhedral Meshes with Mixed Cells"

Vladimir Gvozdev[†]

Yuri Kuznetsov [†]

Mikhail Shashkov [††]

[†]Department of Mathematics, University of Houston

[††]Los Alamos National Laboratory

2006

Contents

1 Introduction

In this Report, we describe a new mimetic finite-difference method for the diffusion equations on polygonal/polyhedral meshes when the coefficients and the right-hand side of the equations are discontinuous inside mesh cells. The latter situation occurs in many important practical applications when a designed mesh does not fit the interfaces between different materials. The proposed method can be also efficiently applied to the case of meshes with strong refinement in local subdomains and to homogenization problems. The new method allows to reduce significantly the size of the underlying algebraic systems by using special elimination procedures for groups of interior DOF.

The Report is organized as follows. In Section 2, we give the formulation of the problem. In Section 3, we describe in details the proposed method. In Section 4, we give the algebraic analysis of the method. Section 5 contains results of numerical experiments. Finally, in Section 6, we briefly indicate two natural generalizations of the new method.

2   Problem formulation

2.1   Differential formulation

We consider the diffusion equation

$$-\operatorname{div}\left(a\operatorname{grad}p\right) + cp = f \quad\text{in}\quad \Omega \tag{1}$$

where p is an unknown scalar solution function (pressure), $a = a(x)$ is a diffusion tensor, $c = c(x) \in L_\infty(\Omega)$ is a nonnegative function, $f = f(x) \in L_2(\Omega)$ is a source function, and $\Omega \subset \mathbb{R}^2$ is a bounded domain. We assume that the boundary $\partial\Omega$ of the domain Ω is partitioned into two nonoverlapping sets Γ_D (Dirichlet) and Γ_N (Neumann), such that $\Gamma_D = \overline{\Gamma}_D$ and $\overline{\Gamma_D \cup \Gamma_N} = \partial\Omega$.

In general, we assume that a is a symmetric, uniformly positive definite 2×2 matrix which piecewise constant entries, i.e.

$$\left(a(x)\boldsymbol{\xi},\ \boldsymbol{\xi}\right) \geq \alpha^2\left(\boldsymbol{\xi},\ \boldsymbol{\xi}\right) \quad \forall\boldsymbol{\xi} \in \mathbb{R}^2 \ \text{ a.e. in } \overline{\Omega}$$

with a positive constant α^2 which is independent of x and $\boldsymbol{\xi}$.

Equation (1) is complemented with the boundary conditions

$$\begin{aligned}
p &= g_D &&\text{on}\quad \Gamma_D, \\
\left(a\operatorname{grad}p\right)\cdot\boldsymbol{n} &= g_N &&\text{on}\quad \Gamma_N,
\end{aligned} \tag{2}$$

where $\boldsymbol{n}$ is the outward unit normal vector to $\partial\Omega$, g_D and g_N are given functions on Γ_D and Γ_N, respectively. We assume that problem (1) - (2) has a solution $p = p^*(x)$.

We replace differential problem (1)-(2) by the equivalent first order system

$$
\begin{aligned}
a^{-1}\boldsymbol{u} \;+\; \operatorname{grad} p \;&=\; 0 \\
\operatorname{div} \boldsymbol{u} \;+\; c\,p \;&=\; f \quad \text{in} \quad \Omega
\end{aligned}
\tag{3}
$$

with boundary conditions

$$
\begin{aligned}
p \;&=\; g_D \quad \text{on} \quad \Gamma_D, \\
-\boldsymbol{u}\cdot\boldsymbol{n} \;&=\; g_N \quad \text{on} \quad \Gamma_N,
\end{aligned}
\tag{4}
$$

where $\boldsymbol{u} = -a\operatorname{grad} p$ denotes the unknown flux vector function.

2.2 Mimetic finite difference method

Let $\mathcal{T}_h$ be a triangular partitioning of Ω. This partitioning can be, generally speaking, nonconforming, i.e. a vertex of a mesh triangle in $\mathcal{T}_h$ may belong to the interior of an edge of another triangle in $\mathcal{T}_h$. We define the scalar product in the space of discrete normal fluxes with a symmetric positive definite matrix M (see, for instance, [2], [4]). Then the mimetic finite-difference discretization of (3)-(4) is defined by the system of mesh equations

$$
\begin{aligned}
\boldsymbol{u}_h \;+\; \mathrm{GRAD}_h\, p_h &= 0 \\
\mathrm{DIV}_h\, \boldsymbol{u}_h \;+\; c_h\, p_h &= f_h
\end{aligned}
\tag{5}
$$

with properly defined discrete boundary conditions. This mesh system can be presented in the matrix form by

$$
\begin{pmatrix} M & B^T \\ B & -\Sigma \end{pmatrix} \begin{pmatrix} \bar{u} \\ \bar{p} \end{pmatrix} = \begin{pmatrix} \bar{G} \\ \bar{F} \end{pmatrix}
\tag{6}
$$

with properly defined matrices M (matrix of the scalar products in the space of fluxes), B, and Σ and vectors $\bar{G}$ and $\bar{F}$.

2.3 Connection with mixed FE method

The weak formulation of (3) - (4) is as follows [1]: find $\boldsymbol{u} \in H(\mathrm{div},\ \Omega)$, $\boldsymbol{u} \cdot \boldsymbol{n} = -g_N$ on Γ_N, and $p \in L_2(\Omega)$ such that the equations

$$
\begin{aligned}
a(\boldsymbol{u}, \boldsymbol{v}) &+& b(\boldsymbol{v}, p) &=& l_D(\boldsymbol{v}) \\
b(\boldsymbol{u}, q) &-& \sigma(p, q) &=& l_f(q)
\end{aligned}
\tag{7}
$$

hold true for all $\boldsymbol{v} \in H(\mathrm{div},\ \Omega)$, $\boldsymbol{v} \cdot \boldsymbol{n} = 0$ on Γ_N, and $q \in L_2(\Omega)$.

Here the bilinear forms and linear functionals are defined by

$$
\begin{aligned}
a(\boldsymbol{u}, \boldsymbol{v}) &= \int_\Omega \left(a^{-1}\boldsymbol{u}\right) \cdot \boldsymbol{v}\, \mathrm{dx}, & b(\boldsymbol{u}, q) &= -\int_\Omega \mathrm{div}\,\boldsymbol{u}\, q\, \mathrm{dx}, \\
\sigma(p, q) &= \int_\Omega c\, p\, q\, \mathrm{dx}, & & \\
l_D(\boldsymbol{v}) &= -\int_{\Gamma_D} g_D(\boldsymbol{v} \cdot \boldsymbol{n})\, \mathrm{ds}, & l_f(q) &= -\int_\Omega f\, q\, \mathrm{dx}.
\end{aligned}
\tag{8}
$$

In order to approximate the above problem, we apply the mixed finite element method. Given the finite dimensional subspaces $\boldsymbol{V}_h$ of the space of fluxes $\boldsymbol{V} \equiv H(\mathrm{div}, \Omega)$, and Q_h of the space of pressures $Q \equiv L_2(\Omega)$, respectively, we introduce the finite element problem in the form:
find $\boldsymbol{u}_h \in \boldsymbol{V}_h$, $\boldsymbol{u}_h \cdot \boldsymbol{n} = -g_{N,h}$ on Γ_N, and $p_h \in Q_h$ such that the equations

$$
\begin{aligned}
a(\boldsymbol{u}_h, \boldsymbol{v}) \;+\; b(\boldsymbol{v}, p_h) &= l_D(\boldsymbol{v}) \\[2mm]
b(\boldsymbol{u}_h, q) \;-\; \sigma(p_h, q) &= l_f(q)
\end{aligned}
\tag{9}
$$

hold true for all $\boldsymbol{v} \in \boldsymbol{V}_h$, $\boldsymbol{v} \cdot \boldsymbol{n} = 0$ on Γ_N, and $q \in Q_h$. Here $g_{N,h}$ is an appropriate approximation of the function g_N on Γ_N.

Mixed FE method generates the mass matrix M which defines the scalar product in the space of discrete normal fluxes. If we choose the space $\boldsymbol{V}_h$ in (9) as described in Section 3, and we choose the underlying mass matrix M for the scalar product in the mimetic finite-difference method then both methods result in the same algebraic system (6).

2.4 Assumptions

For the sake of simplicity, we assume that Ω is a union of L nonoverlapping polygons Ω_l with boundaries $\partial\Omega_l$, i.e.

$$\bar{\Omega} = \bigcup_{l=1}^{L} \bar{\Omega}_l. \tag{10}$$

Thus, Ω is a polygon with polygonal subdomains Ω_l, $l = \overline{1, L}$.

Also, for the sake of simplicity, we assume that in each subdomain Ω_l the coefficient c is a positive constant and a is a constant scalar tensor, i.e.

$$c \equiv c_l \quad \text{and} \quad a = a_l\, I_2 \quad \text{in} \quad \Omega, \tag{11}$$

where c_l and a_l are positive constants, $l = \overline{1, L}$, and I_2 is the identity 2×2 matrix.

3 Mimetic finite-difference method on polygonal meshes with mixed cells

3.1 Polygonal meshes with mixed cells

Let $\mathcal{T}_H(\Omega) = \{E_k\}_{k=1}^N$ be a conforming partition of Ω into nonoverlapping polygons, i.e.

$$\overline{\Omega} = \bigcup_{k=1}^N E_k, \quad \text{int } E_k \bigcap \text{int } E_l = \emptyset, \quad l \neq k. \tag{12}$$

where int E_k denotes the interior of E_k.

The term "conforming" implies that two different polygons in the partition have either a common vertex, or a common whole edge, or a common whole face, or do not intersect. We also assume that if f is a boundary face of E_k for some k (i.e. $f \subset \partial\Omega$) then either $f \subset \Gamma_D$, or $f \subset \Gamma_N$.

A mesh cell E_k is said to be mixed if the interior of E_k has nonempty intersections with at least two subdomains Ω_l with different values of a_l and/or c_l, $l = \overline{1, L}$. If the partitioning $\mathcal{T}_H$ is not conforming with respect to the boundaries of subdomains Ω_l we definitely get mixed mesh cells E_k, $1 \leq k \leq N$. Two examples of a mixed square mesh cell are shown in Figures 1 and 2.
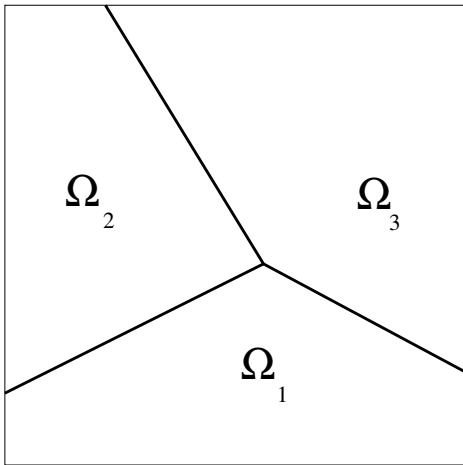
Figure 1: Mixed cell with three materials
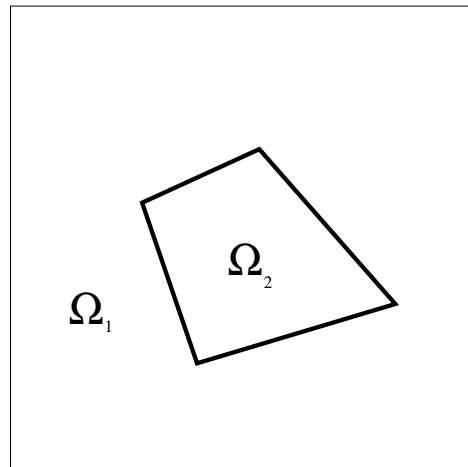
Figure 2: Mixed cell with inclusion

3.2   Triangulation of mesh cells E_k

Let E be a particular mesh cell E_k in $\mathcal{T}_H$ with $m \equiv m_k$ edges Γ_s, $s = \overline{1, m}$. For example, for square mesh cells in Figures 1 and 2, $m = 4$. If the boundary ∂E of E intersects at least one of the interfaces between subdomains Ω_l and $\Omega_{l'}$, $l \neq l'$, this mesh cell is mixed. For instance, in Figure 1, three faces of E intersect interface boundaries between subdomains Ω_1, Ω_2, and Ω_3. The mesh cell in Figure 2 is mixed but its boundary does not intersect with interfaces between subdomains.

We define a partitioning of ∂E into T segments γ_t, $t = \overline{1, T}$ such that the interior of each segment γ_t belongs either to the interior of one subdomain Ω_l, $l = \overline{1, L}$, or to the interface boundary between only two subdomains Ω_l and $\Omega_{l'}$, $1 \leq l < l' \leq L$, or to $\Gamma_N \cap \partial\Omega_l$, $1 \leq l \leq L$. Thus,

$$\partial E = \bigcup_{t=1}^{T} \gamma_t. \tag{13}$$

For example, for the mesh cell E in Figure 1 the boundary ∂E is partitioned into seven segments $\{\gamma_t\}$, i.e. $T = 7$.

Let $\mathcal{T}_{E,h}$ be a conforming partitioning of E into n triangles e_j, i.e.

$$E = \bigcup_{j=1}^{n} e_j. \tag{14}$$

The conformity of triangulation means that any two different triangles in $\mathcal{T}_{E,h}$ either have a common edge, or a common vertex, or do not intersect each other.

We assume that the partitioning $\mathcal{T}_{E,h}$ is also conforming with respect to interface boundaries between subdomains Ω_l and $\Omega_{l'}$, $1 \leq l < l' \leq L$, i.e. edges of triangles in $\mathcal{T}_{e,h}$ do not intersect these interfaces. Examples of $\mathcal{T}_{E,h}$ for the cell E in Figures 1 and 2 are shown in Figures 3 and 4, respectively.
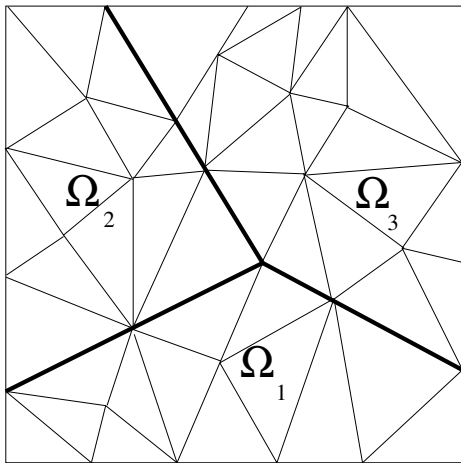
Figure 3: An example of $\mathcal{T}_{E,h}$
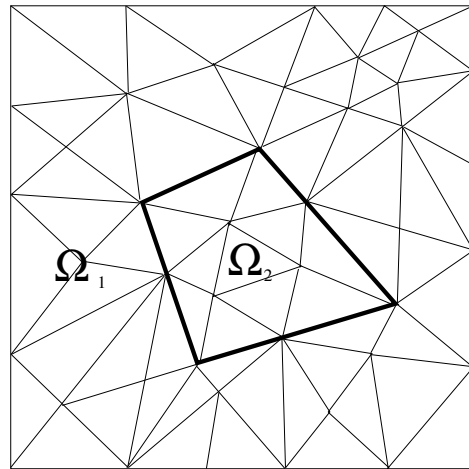
Figure 4: An example of $\mathcal{T}_{E,h}$

We define the global triangular partitioning $\mathcal{T}_h$ of Ω by

$$\mathcal{T}_h \;=\; \mathcal{T}_{E_k,h} \quad \text{on} \quad E_k, \quad k = \overline{1,\ N},$$

i.e. the trace of $\mathcal{T}_h$ on a mesh cell E_k is the above triangulation $\mathcal{T}_{E_k,h}$ of E_k, $k = \overline{1,\ N}$. It is obvious that the triangulation $\mathcal{T}_h$ is not globally conforming if the triangulations $\mathcal{T}_{E_k,h}$ and $\mathcal{T}_{E_{k'},h}$ do not match on the interfaces between cells E_k and $E_{k'}$, $1 \leq k < k' \leq N$.

The major goal of this research is to construct a discretization for the diffusion problem (1) - (2) under the following conditions:

1. all the degrees of freedom (DOF) for the flux $\boldsymbol{u}$ should be associated with the interface segments $\gamma_{k,t} = \gamma_{k',t'}$ between neighboring cells E_k and $E_{k'}$ with only one DOF per interface segment;

2. all the DOF representing the solution function p should be associated with cells E_k in $\mathcal{T}_H$ with only one DOF per E_k, $k = \overline{1, \ N}$

The discretization method to be proposed consists of four steps:

1. we derive a discretization for the second equation in (3) (the conservation law equation) on E_k, $k = \overline{1, \ N}$;

2. we discretize problem (3) - (4) by a mimetic finite-difference method on triangular mesh $\mathcal{T}_h$;

3. we eliminate the DOF for the flux $\boldsymbol{u}$ associated with the edges of $\mathcal{T}_h$ which are interior for cells E_k, $k = \overline{1, \ N}$. We also eliminate all the DOF for the solution function p;

4. we derive the requested discretization by the combining of the discrete equations obtained in steps 1 and 3

Step 1

We derive the discretization for the conservation law equation by the integration of this equation over the cells E_k in $\mathcal{T}_H$:

$$\int\limits_{E_k} \left(\nabla\!\cdot\!\boldsymbol{u} + c\,p\right) \mathrm{dx} \;\equiv\; \sum_{t=1}^{T_k} \int\limits_{\gamma_{k,t}} \left(\boldsymbol{u}\!\cdot\!\boldsymbol{n}_{k,t}\right) \mathrm{ds} + \int\limits_{E_k} c\,p\,\mathrm{dx} \;=\; \int\limits_{E_k} f\,\mathrm{dx}, \quad k = \overline{1,\ N}, \tag{15}$$

where $\boldsymbol{n}_{k,t}$ is a unit normal to $\gamma_{k,t}$, $t = \overline{1,\ T_k}$. If $\gamma_{k,t}$ belongs to interface between E_k and a neighboring cell $E_{k'}$, and $k < k'$, we assume that $\boldsymbol{n}_{k,t}$ is directed from E_k into $E_{k'}$. On $\gamma_{k,t}$ belonging to $\partial\Omega$, we assume that $\boldsymbol{n}_{k,t}$ is the unit outward normal to $\partial\Omega$.

Thus, the discrete equation for E_k can be written as

$$\sum_{t=1}^{T_k} |\gamma_{k,t}|u_{k,t} \;+\; |E_k|\,\hat{c}_k\,p_k \;=\; |E_k|\,f_k \tag{16}$$

where $|\gamma_{k,t}|$ is the length of $\gamma_{k,t}$, $|E_k|$ is the area of E_k,

$$\hat{c}_k \;=\; \frac{1}{|E_k|} \int\limits_{E_k} c\,\mathrm{dx}, \quad f_k \;=\; \frac{1}{|E_k|} \int\limits_{E_k} f\,\mathrm{dx}, \tag{17}$$

and

$$u_{k,t} \;=\; \frac{1}{|\gamma_{k,t}|} \int\limits_{\gamma_{k,t}} \left(\boldsymbol{u} \cdot \boldsymbol{n}_{k,t}\right) \mathrm{ds}. \tag{18}$$

The equations (15) are complemented by the conditions that on the interface segments $\gamma_{k',t'} = \gamma_{k,t}$ between neighboring cells E_k and $E_{k'}$ with $k < k'$ we have

$$u_{k',t'} \;=\; -\,u_{k,t}. \tag{19}$$

16

Step 2

Let $\boldsymbol{W}_{k,h}$ be the lowest order Raviart-Thomas FE space on the triangulation $\mathcal{T}_{E_k,h}$, $k = \overline{1,\ N}$. Then the FE space $\boldsymbol{V}_h$ for the mixed FE method (9) is defined as follows. $\boldsymbol{V}_h$ consists of vector functions $\boldsymbol{v}_h$ such that:

1. $\boldsymbol{v}_h \in \boldsymbol{W}_{k,h}$ in E_k, $k = \overline{1,\ N}$;

2. $\boldsymbol{v}_h \cdot \boldsymbol{n}_{k,t} \equiv v_{k,t} = \text{const}$ on $\gamma_{k,t}$ under the condition (19), $t = \overline{1,\ T_k}$, $k = \overline{1,\ N}$.

The latter choice of $\boldsymbol{V}_h$ generates the symmetric positive definite matrices M_k, $k = \overline{1,\ N}$, and M for the polygonal cells E_k, $k = \overline{1,\ N}$, and for the whole domain Ω, respectively. With the above matrix M for the scalar product in the space of discrete fluxes the mimetic finite-difference method (5) results in system (6) with the matrix

$$\mathcal{A} \equiv \begin{pmatrix} M & B^T \\ B & -\Sigma \end{pmatrix} = \sum_{k=1}^{N} \mathcal{N}_k\, A_k\, \mathcal{N}_k^T \tag{20}$$

where

$$A_k = \begin{pmatrix} M_k & B_k^T \\ B_k & -\Sigma_k \end{pmatrix} \tag{21}$$

is the matrix derived in E_k on the triangular mesh $\mathcal{T}_{E_k,h}$ by the mimetic finite-difference method with the scalar product matrix M_k, and $\mathcal{N}_k$ is the assembling matrix, $k = \overline{1,\ N}$.

Step 3

In order to describe the elimination algorithm for the vector $\bar{p}$ and the interior (with respect to mesh cells E_k, $k = \overline{1, \ N}$) DOF for the flux $\bar{u}$ we introduce the following partitionings for the vectors $\bar{u}$ and $\bar{G}$, and the matrices M and B in (6):

$$
\bar{u} = \begin{pmatrix} \bar{u}_\Gamma \\ \bar{u}_i \end{pmatrix}, \quad \bar{G} = \begin{pmatrix} \bar{G}_\Gamma \\ \bar{G}_i \end{pmatrix},
$$

$$
M = \begin{pmatrix} M_\Gamma & M_{\Gamma i} \\ M_{i\Gamma} & M_i \end{pmatrix}, \quad B = \begin{pmatrix} B_\Gamma & B_i \end{pmatrix},
$$

(22)

where subindex "i" stays for the interior DOF of $\bar{u}$, and "Γ" stays for the rest of DOF which are associated with boundaries ∂E_k of E_k, $k = \overline{1, \ N}$.

With the above partitionings, we can present system (6) in the following block form

$$
\begin{pmatrix} M_\Gamma & M_{\Gamma i} & B_\Gamma^T \\ M_{i\Gamma} & M_i & B_i^T \\ B_\Gamma & B_i & -\Sigma \end{pmatrix} \begin{pmatrix} \bar{u}_\Gamma \\ \bar{u}_i \\ \bar{p} \end{pmatrix} = \begin{pmatrix} \bar{G}_\Gamma \\ \bar{G}_i \\ \bar{F} \end{pmatrix}.
$$

(23)

First, we eliminate the subvector $\bar{u}_i$. Then we get the system

$$
\begin{pmatrix} \widetilde{M}_\Gamma & \widetilde{B}_\Gamma^T \\ \widetilde{B}_\Gamma & -S \end{pmatrix} \begin{pmatrix} \bar{u}_\Gamma \\ \bar{p} \end{pmatrix} = \begin{pmatrix} \bar{g}_\Gamma \\ \bar{f} \end{pmatrix}
$$

(24)

where

$$
\widetilde{M}_\Gamma = M_\Gamma - M_{\Gamma i} M_i^{-1} M_{i\Gamma}
$$

(25)

is the Schur complement for matrix M,

$$
\widetilde{B}_\Gamma = B_\Gamma - B_i M_i^{-1} M_{i\Gamma},
$$

(26)

$$S = B_i \, M_i^{-1} \, B_i^T + \Sigma, \tag{27}$$

$$\bar{f} = \bar{F} - B_i \, M_i^{-1} \, \bar{G}_i, \tag{28}$$

and

$$\bar{g}_\Gamma = \bar{G}_\Gamma - M_{\Gamma i} \, M_i^{-1} \, \bar{G}_i. \tag{29}$$

It is obvious that both matrices $\widetilde{M}_\Gamma$ and S are symmetric and positive definite. Moreover, S is a block diagonal matrix.

Let us introduce the partitionings for the matrices M_k and B_k similar to those we defined for the matrices M and B in (22):

$$M_k = \begin{pmatrix} M_\Gamma^{(k)} & M_{\Gamma i}^{(k)} \\ M_{i\Gamma}^{(k)} & M_i^{(k)} \end{pmatrix}, \quad B_k = \begin{pmatrix} B_\Gamma^{(k)} & B_i^{(k)} \end{pmatrix}, \quad k = \overline{1, \ N}. \tag{30}$$

Then, the matrices $\widetilde{M}_\Gamma$, $\widetilde{B}_\Gamma$, and S in (25)-(27) can be presented in the assembling form as follows:

$$\widetilde{M}_\Gamma = \sum_{k=1}^N N_{\Gamma,k} \, \widetilde{M}_\Gamma^{(k)} \, N_{\Gamma,k}^T, \tag{31}$$

$$\widetilde{B}_\Gamma = \sum_{k=1}^N N_{S,k} \, \widetilde{B}_\Gamma^{(k)} \, N_{\Gamma,k}^T, \tag{32}$$

and

$$S = \sum_{k=1}^N N_{S,k} \, S_k \, N_{S,k}^T \tag{33}$$

with the appropriate assembling matrices $N_{\Gamma,k}$ and $N_{S,k}$, $k = \overline{1, \ N}$.

Here,

$$\widetilde{M}_{\Gamma}^{(k)} = M_{\Gamma}^{(k)} - M_{\Gamma i}^{(k)} \left[M_i^{(k)} \right]^{-1} M_{i\Gamma}^{(k)} \tag{34}$$

$$\widetilde{B}_{\Gamma}^{(k)} = B_{\Gamma}^{(k)} - B_i^{(k)} \left[M_i^{(k)} \right]^{-1} M_{i\Gamma}^{(k)}, \tag{35}$$

and

$$S_k = B_i^{(k)} \left[M_i^{(k)} \right]^{-1} \left[B_i^{(k)} \right]^T + \Sigma_k. \tag{36}$$

Thus, the matrices in (31)-(33) can be computed on the element-by-element basis by computing the matrices in (34)-(36) in parallel.

Now, we get the system for the flux DOF by eliminating the vector $\bar{p}$ in (24):

$$R \, \bar{u}_{\Gamma} = \bar{\xi}_{\Gamma} \tag{37}$$

where

$$R = \widetilde{M}_{\Gamma} + \widetilde{B}_{\Gamma}^T \, S^{-1} \, \widetilde{B}_{\Gamma} \tag{38}$$

and

$$\bar{\xi}_{\Gamma} = \bar{g}_{\Gamma} + \widetilde{B}_{\Gamma}^T \, S^{-1} \, \bar{f}. \tag{39}$$

As it was mentioned before, S is a block diagonal matrix with the matrices S_k on the diagonal, $k = \overline{1, \, N}$.

Step 4

Now, we shall derive the final system by using equations (16)-(19) and (37)-(39). For this goal, we present equation (16) assigned for a cell E_k in the following matrix form:

$$\widehat{B}_\Gamma^{(k)}\, \bar{u}_\Gamma \;-\; \sigma_k\, p_k \;=\; |E_k|\, f_k, \tag{40}$$

where

$$\sigma_k \;=\; |E_k|\, \hat{c}_k, \tag{41}$$

$1 \le k \le N$. At the same time, the equations in (23) assigned for the cell E_k can be written in the matrix form by:

$$B_\Gamma^{(k)}\, \bar{u}^{(k)} \;-\; \Sigma_k\, \bar{p}^{(k)} \;=\; \bar{F}^{(k)} \tag{42}$$

where $\bar{u}^{(k)}$, $\bar{p}^{(k)}$, and $\bar{F}^{(k)}$ are the restrictions on E_k of the vectors $\bar{u}$, $\bar{p}$, and $\bar{F}$, respectively.

Let us denote by $\bar{e}_k$ the column-vector in $\mathbb{R}^{n_k}$ with all the components equal to one, i.e.

$$\bar{e}_k^T \;=\; \begin{pmatrix} 1 & 1 & \ldots & 1 \end{pmatrix}. \tag{43}$$

Let us also denote the diagonal entries of the diagonal matrix Σ_k by $\sigma_i^{(k)}$, $i = \overline{1,\ n_k}$, i.e.

$$\Sigma_k \;=\; \operatorname{diag}\left\{ \sigma_1^{(k)},\ \sigma_2^{(k)},\ \ldots,\ \sigma_{n_k}^{(k)} \right\}. \tag{44}$$

It can be easily shown that equation (40) can be obtained by multiplication of equation (42) by the vector $\bar{e}_k^T$. In particular,

$$\widehat{B}_\Gamma^{(k)} \;=\; P_k \begin{pmatrix} \bar{e}_k^T\, B_\Gamma^{(k)} & 0 \end{pmatrix} \bar{P}_k^T \tag{45}$$

where P_k is the appropriate permutation matrix,

$$\sigma_k \;=\; \sum_{i=1}^{n_k} |e_i^{(k)}|\, c_i^{(k)}, \tag{46}$$

$$\bar{p}^{(k)} = \frac{1}{\sigma_k} \sum_{i=1}^{n_k} |e_i^{(k)}| \, c_i^{(k)} \, p_i^{(k)}, \tag{47}$$

and

$$\bar{f}^{(k)} = \frac{1}{|E_k|} \sum_{i=1}^{n_k} |e_i^{(k)}| \, c_i^{(k)} \, f_i^{(k)}, \tag{48}$$

where

$$c_i^{(k)} = \frac{1}{|e_i^{(k)}|} \int_{e_i^{(k)}} c \, \mathrm{dx}, \tag{49}$$

and

$$f_i^{(k)} = \frac{1}{|e_i^{(k)}|} \int_{e_i^{(k)}} f \, \mathrm{dx}, \tag{50}$$

$1 \le i \le n_k$, $1 \le k \le N$.

Thus, we have arrived to two systems of equations

$$R \, \bar{u}_\Gamma = \bar{\xi} \tag{51}$$

$$\widehat{B}_\Gamma \, \bar{u}_\Gamma - \widehat{\Sigma} \, \bar{p}_E = \bar{F}_E \tag{52}$$

where the rows of $\widehat{B}_\Gamma$ are defined in (15),

$$\widehat{\Sigma} = \mathrm{diag} \left\{ \sigma_1, \ \sigma_2, \ \dots, \ \sigma_N \right\}, \tag{53}$$

and components of $\bar{p}_E$ and $\bar{F}_E$ are defined in (47) and (48), respectively.

We derive the final system

22

$$\widehat{M}\,\bar{u}_\Gamma \;+\; \widehat{B}_\Gamma^T\,\bar{p}_E \;=\; \bar{\eta}$$
$$\widehat{B}_\Gamma\,\bar{u}_\Gamma \;-\; \widehat{\Sigma}\,\bar{p}_E \;=\; \bar{F}_E \tag{54}$$

where

$$\widehat{M} \;=\; R \;-\; \widehat{B}_\Gamma^T\,\widehat{\Sigma}^{-1}\,\widehat{B}_\Gamma \tag{55}$$

and

$$\bar{\eta} \;=\; \bar{\xi} \;-\; \widehat{B}_\Gamma^T\,\widehat{\Sigma}^{-1}\,\bar{F}_E. \tag{56}$$

In fact, we multiply equations in system (52) by the matrix $\widehat{B}_\Gamma^T\widehat{\Sigma}^{-1}$ and subtract them from the the equations in system (51) .

It can be shown by using special algebraic analysis that matrix $\widehat{M}$ in (55) is positive definite and well conditioned. For instance, its minimal eigenvalue is bounded from below by the minimal eigenvalue of matrix M in (20).

4 Algebraic analysis of the method

Let us consider the following eigenvalue problem for the matrix S_k in (36):

$$S \, \bar{w} \; \equiv \; \left(B_i \, M_i^{-1} \, B_i^T \; + \; \Sigma \right) \bar{w} \; = \; \lambda \, \bar{w} \tag{57}$$

where, for the sake of simplicity, the upper index "k" is omitted.

Then, the spectral decomposition of S is given by

$$S \; = \; \Sigma \, W \, \Lambda \, W^T \, \Sigma \tag{58}$$

where

$$\begin{aligned} \Lambda &= \; \mathrm{diag}\{\lambda_1, \; \lambda_2, \; \ldots \; , \; \lambda_n\}, \\ W &= \; \left[\bar{w}_1, \; \bar{w}_2, \; \ldots \; , \; \bar{w}_n \right], \end{aligned} \tag{59}$$

and n is the size of S. Here, $1 = \lambda_1 < \lambda_2 \leq \cdots \leq \lambda_n$ are the eigenvalues in (57) and $\bar{w}_1, \bar{w}_2, \ldots, \bar{w}_n$ are the underlying Σ-orthonormalized eigenvectors, i.e.

$$(\bar{w}_k, \; \bar{w}_l)_\Sigma \; \equiv \; (\Sigma \, \bar{w}_k, \; \bar{w}_l) \; = \; \delta_{kl}, \quad k, l = \overline{1, \; n}, \tag{60}$$

and δ_{kl} is the Kronecker delta.

The kernel of B_i consists of the vectors with equal components. Thus, the dimension of $\ker (S - \Sigma)$ equals one. It follows that the minimal eigenvalue $\lambda_1 = 1$ of S is single, i.e. $\lambda_1 < \lambda_2$, and the underlying eigenvector $\bar{w}_1$ in (57) is known explicitly:

$$\bar{w}_1 \; = \; \beta \, \bar{e} \tag{61}$$

where

$$\bar{e} \; = \; \begin{pmatrix} 1 & \cdots & 1 \end{pmatrix}, \tag{62}$$

24

$$\beta^2 \;=\; \frac{1}{(\Sigma\,\bar{e},\;\bar{e})} \;=\; \frac{1}{\sigma}, \tag{63}$$

and σ is defined in (41), (46),(49):

$$\sigma \;=\; |E|\,\hat{c}. \tag{64}$$

Remind that the index "k" is omitted for the sake of simplicity in notations.

The spectral decomposition for the matrix S^{-1} can be given by

$$S^{-1} \;=\; W\,\Lambda^{-1}\,W^T \;=\; \sum_{j=1}^{n} \frac{1}{\lambda_j}\,\bar{w}_j\,\bar{w}_j^T \;=\; Q_1 \;+\; Q_2 \tag{65}$$

where

$$Q_1 \;=\; \bar{w}_1\,\bar{w}_1^T \tag{66}$$

and

$$Q_2 \;=\; \sum_{j=2}^{n} \frac{1}{\lambda_j}\,\bar{w}_j\,\bar{w}_j^T. \tag{67}$$

Let us consider the matrices (the index "k" is now back)

$$L_k \;=\; \big[\widetilde{B}_\Gamma^{(k)}\big]^T\,S_k^{-1}\,\widetilde{B}_\Gamma^{(k)}, \tag{68}$$

$k = \overline{1,\ N}$ in (38):

$$\big[\widetilde{B}_\Gamma\big]^T\,S^{-1}\,\widetilde{B}_\Gamma \;\equiv\; \sum_{k=1}^{n} N_{\Gamma,k}\,L_k\,N_{\Gamma,k}^T. \tag{69}$$

With notations (66), (67), we get

$$L_k \;=\; L_k^{(1)} \;+\; L_k^{(2)} \tag{70}$$

where

$$L_k^{(t)} = \left[\widetilde{B}_\Gamma^{(k)}\right]^T Q_t^{(k)} \widetilde{B}_\Gamma^{(k)}, \quad t = 1, 2. \tag{71}$$

It is obvious that the matrices $L_k^{(t)}$, $t = 1, 2$, are symmetric and at least positive semidefinite.

Let us analyze the matrix

$$L_k^{(1)} = \left[\widetilde{B}_\Gamma^{(k)}\right]^T \bar{w}_1^{(k)} \left[\bar{w}_1^{(k)}\right]^T \widetilde{B}_\Gamma^{(k)} \tag{72}$$

where

$$\widetilde{B}_\Gamma^{(k)} = B_\Gamma^{(k)} - B_i^{(k)} \left[M_i^{(k)}\right]^{-1} M_{i\Gamma}^{(k)}. \tag{73}$$

The vectors $\bar{w}_1^{(k)}$ belong to $\ker \left[B_i^{(k)}\right]^T$, $k = \overline{1, \ N}$. Thus, we get much simpler formulas for the matrices $L_k^{(1)}$:

$$L_k^{(1)} = \left[B_\Gamma^{(k)}\right]^T \bar{w}_1^{(k)} \left[\bar{w}_1^{(k)}\right]^T B_\Gamma^{(k)} = \beta_k^2 \left[\widehat{B}_\Gamma^{(k)}\right]^T \widehat{B}_\Gamma^{(k)} \tag{74}$$

where the matrices $\widehat{B}_\Gamma^{(k)}$ are defined in (45), $k = \overline{1, \ N}$.

Finally, we get a simple formula for the matrix $L^{(1)}$:

$$L^{(1)} \equiv \sum_{k=1}^N N_{\Gamma,k} L_k^{(1)} N_{\Gamma,k}^T = \widehat{B}_\Gamma^T \Sigma^{-1} \widehat{B}_\Gamma. \tag{75}$$

Compare (55), (69), and (75), we conclude that the matrix

$$\widehat{M} \equiv R - \widehat{B}_\Gamma^T \widehat{\Sigma}^{-1} \widehat{B}_\Gamma = \widetilde{M} + L^{(2)} \tag{76}$$

where

$$L^{(2)} = \sum_{k=1}^{N} N_{\Gamma,k} \, L_k^{(2)} \, N_{\Gamma,k}^T, \tag{77}$$

is symmetric and positive definite.

It is also obvious that the minimal eigenvalue of $\widehat{M}$ is bounded from below by the minimal eigenvalue of the matrix M in (20). It can be also shown that the condition number of the matrix $\widehat{M}$ does not depend on the mesh step sizes if the mesh Ω_h is regular shaped and quasiuniform.

5   Numerical results

In this Section, we present the results of numerical experiments for the diffusion equation

$$-\mathrm{div}\big(a\,\mathrm{grad}\ p\big)\ +c\,p\ =\ f \tag{78}$$

in the square domain $\Omega\ =\ (0;\ 1)\times(0;\ 1)$ with a scalar diffusion tensor a, a positive coefficient c, and a given source function f. On each side Γ_i, $1\leq i\leq 4$ of Ω the solution p satisfies either Dirichlet, or Neumann boundary condition, i.e.

$$\begin{aligned}
p\ &=\ g_D \quad \text{on}\quad \Gamma_D, \\
-\big(a\,\mathrm{grad}\ p\big)\cdot\boldsymbol{n}\ &=\ g_N \quad \text{on}\quad \Gamma_N
\end{aligned} \tag{79}$$

where $\boldsymbol{n}$ is the outward unit normal to the boundary $\partial\Omega$.

In the numerical experiments, we assume that Ω is partitioned into nonoverlapping subdomains $\{\Omega_k\}$ and in each of the subdomains the coefficients a and c, and the solution function p are constants. The mesh Ω_H is always a square one. The discretization method is described in Section 3. We compare the numerical results for the new methods with the results obtained on the meshes with the earlier proposed in [3], [4] method which we refer as **div-const** one.

The interfaces $\Gamma_{kl}=\partial\Omega_k\cap\partial\Omega_l$ between subdomains do not belong to the union f the edges of the cells in E_H. So, we naturally get mixed cell in the neighborhood of the interface boundaries Γ_{kl}. We calculate the error of the discrete solutions obtained by the new and by div-const methods by using the reference solution.

We calculate the reference solution numerically by the lowest order Raviart-Thomas mixed finite element method on a very fine triangular mesh ($\sim 10^6$ triangles) which is conforming with respect to the interfaces Γ_{kl}.

Test Example 1

In the first experiment, we partition Ω into two rectangles as shown in Figure 5. The mesh Ω_h is chosen in such a way that the interface Γ_{12} between Ω_1 and Ω_2 crosses the vertical set of cells E as shown in Figure 6.
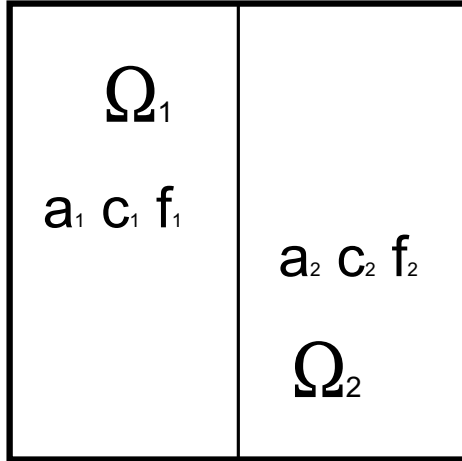
Figure 5: Partitioning of Ω into Ω_1 and Ω_2
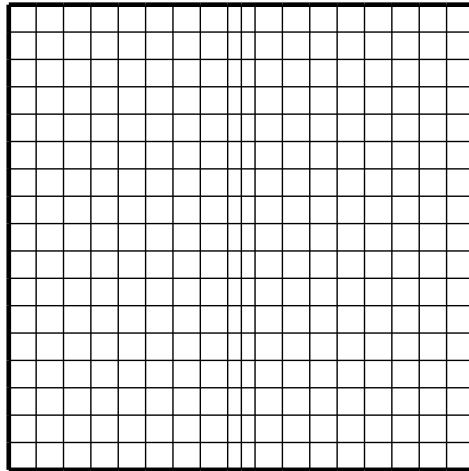
Figure 6: Square mesh Ω_h

Input data:

$$a_1 = 1 \qquad a_2 = 1$$

$$c_1 = 100 \quad c_2 = 0.01$$

$$f_1 = 0.01 \quad f_2 = 100$$

Boundary conditions:

$$p|_{\Gamma_1} = 0$$

$$p|_{\Gamma_2} = 5$$

$$-(a\nabla p \cdot \mathbf{n})|_{\Gamma 3 \cup \Gamma_4} = 0$$

Mesh step size in Ω_h : $h = 1/51$.
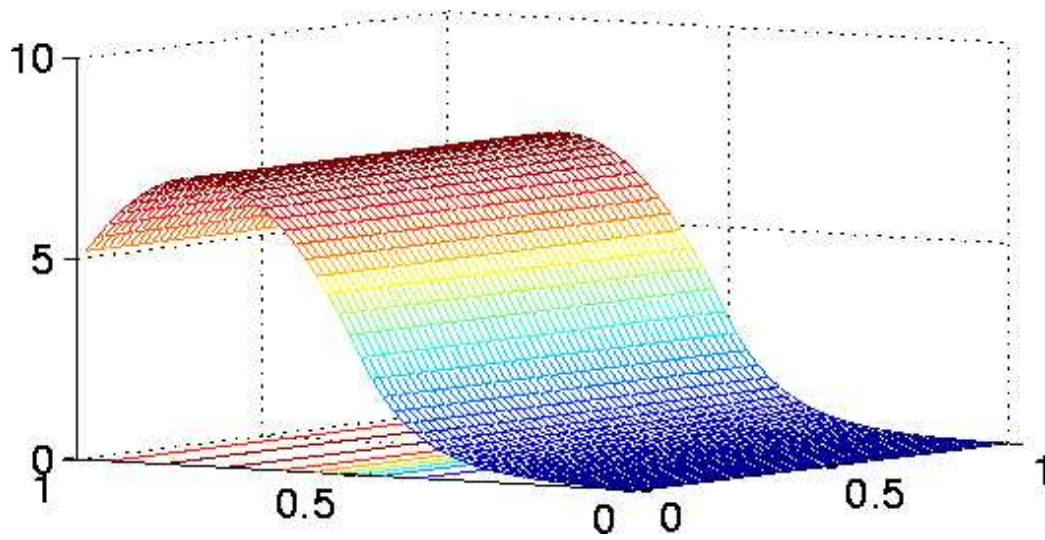
Figure 7: Reference solution
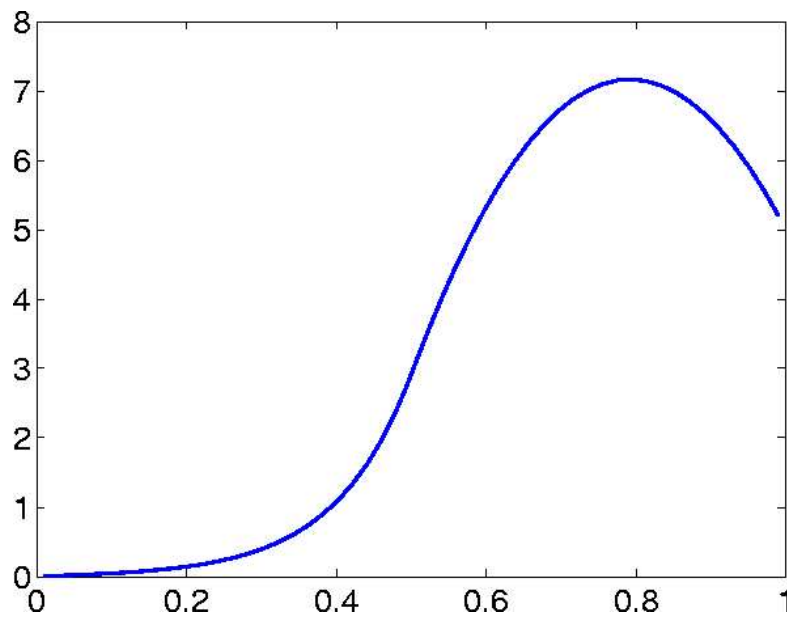
Figure 8: Reference solution along the line y=0.5

31
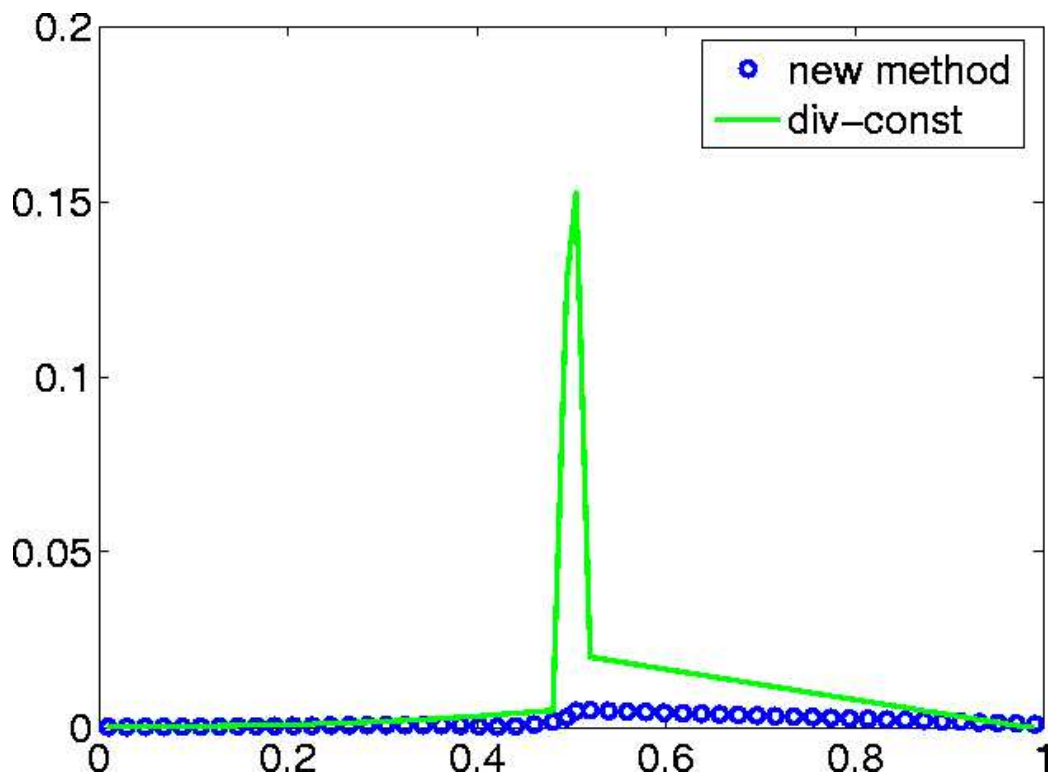
Figure 9: Pointwise error for pressure function along the line y=0.5
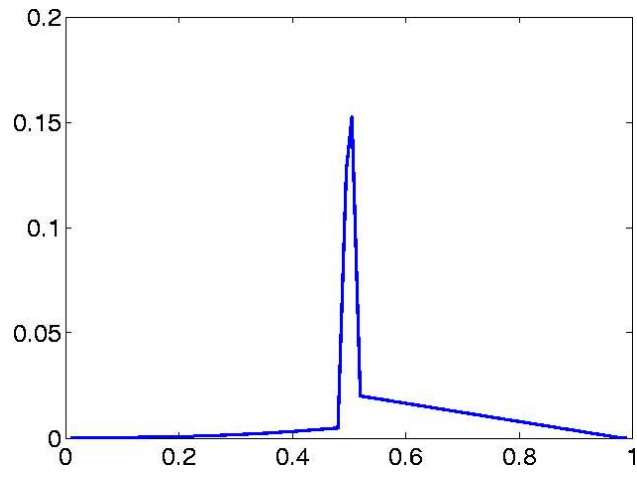
Figure 10: Error for pressure function along the line y=0.5, div-const method
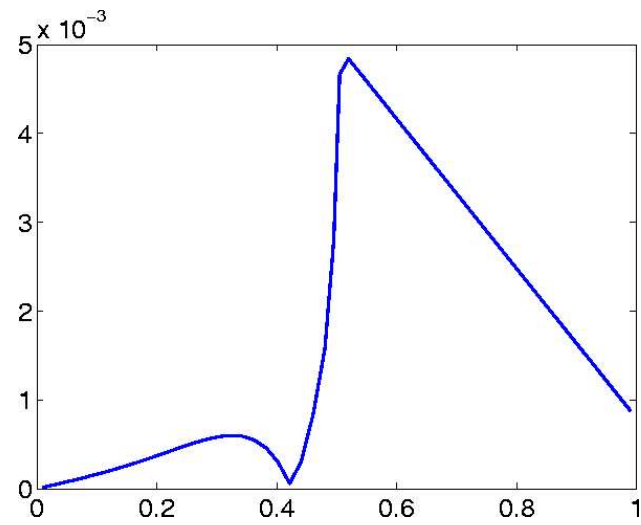
Figure 11: Error for pressure function along the line y=0.5, new method (attention: different scale)
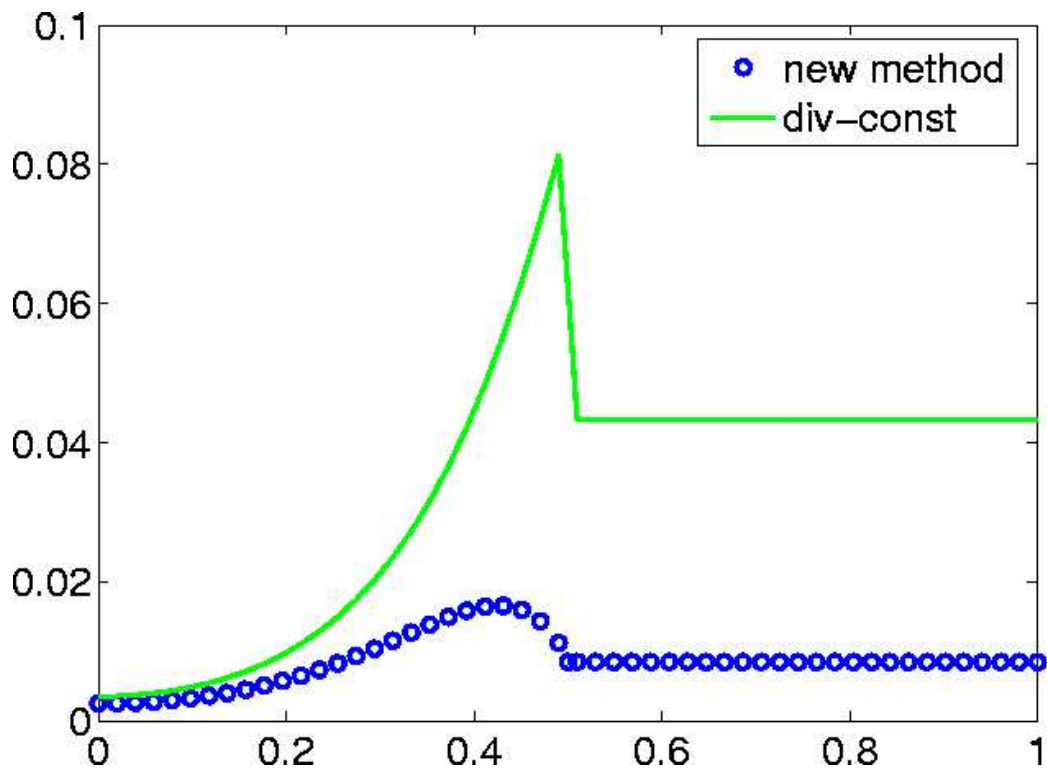
Figure 12: Error for fluxes along the line y=0.5
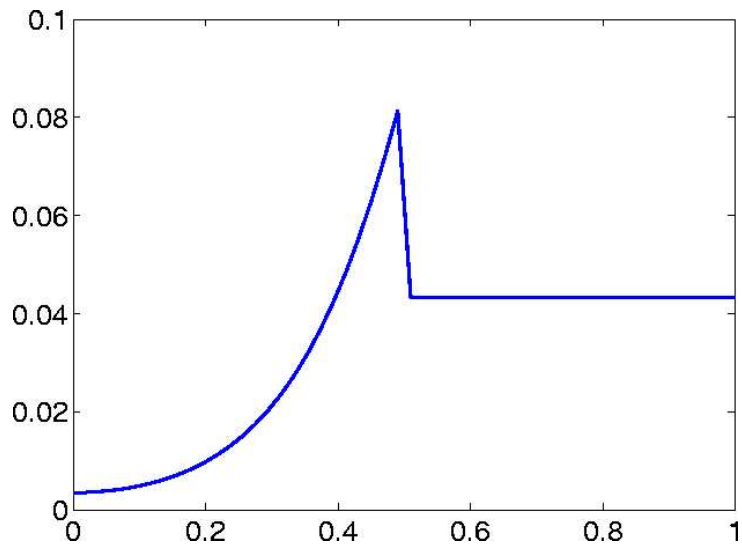
Figure 13: Error for fluxes along the line y=0.5, div-const method
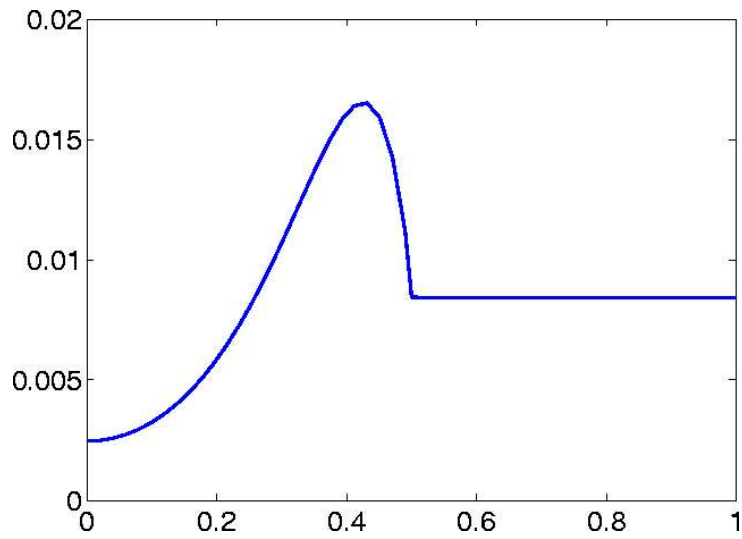
Figure 14: Error for fluxes along the line y=0.5, new method (attention: different scale)

Test Example 2

In the second experiment, we partition Ω into to polyhedrons as shown in Figure 15.
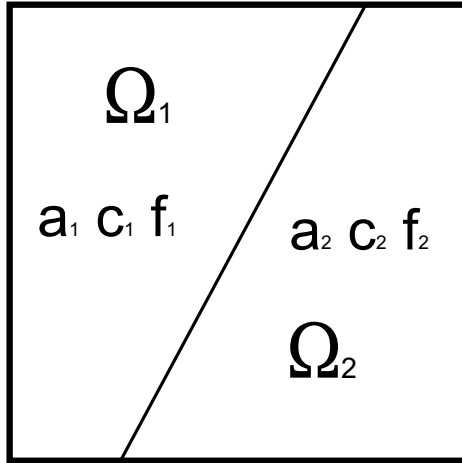
Figure 15: Partitioning of Ω into Ω_1 and Ω_2
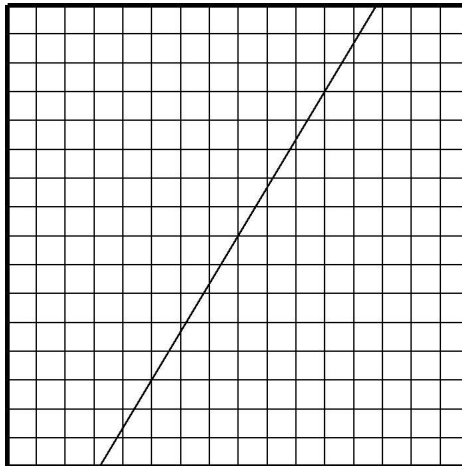
Figure 16: Square mesh Ω_h

Input data:

$$a_1 = 1 \qquad a_2 = 1$$

$$c_1 = 1000 \quad c_2 = 0.01$$

$$f_1 = 0.01 \quad f_2 = 1000$$

Boundary conditions:

$$p|_{\Gamma_1} = 0$$

$$p|_{\Gamma_2} = 10$$

$$-(a\nabla p \cdot \mathbf{n})|_{\Gamma_3 \cup \Gamma_4} = 0$$

Mesh step size in $\Omega_h : h = 1/51$.
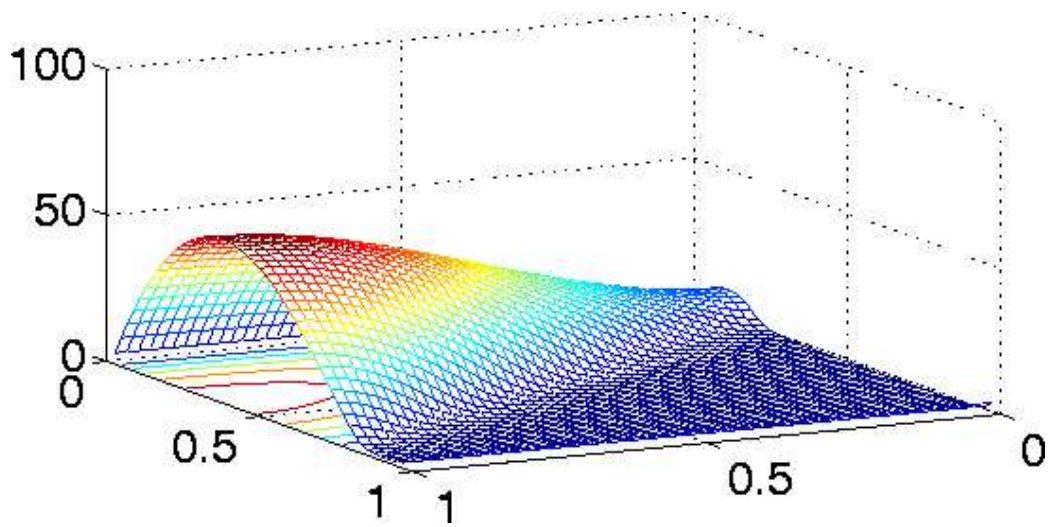
Figure 17: Reference solution
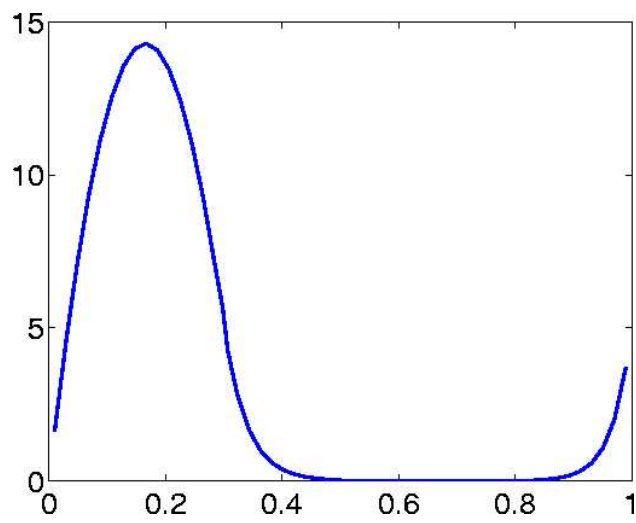
Figure 18: Reference solution along the line y=1/6
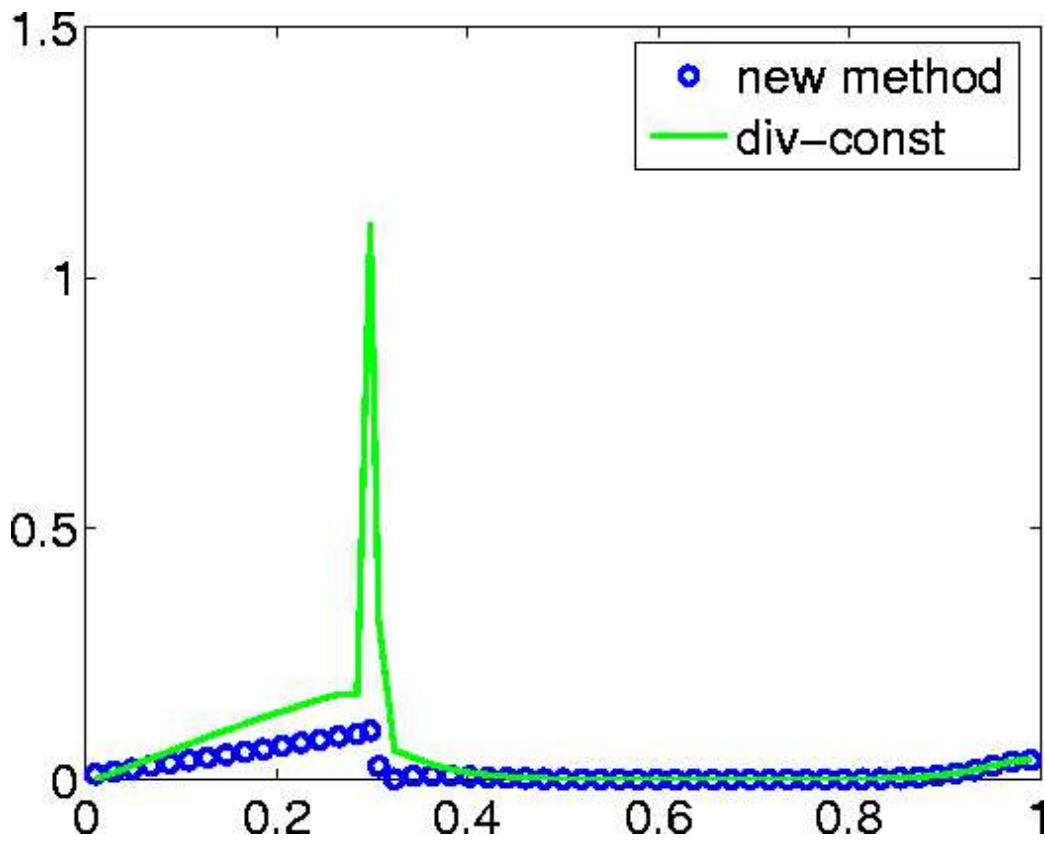
Figure 19: Pointwise error for pressure function along the line y=1/6
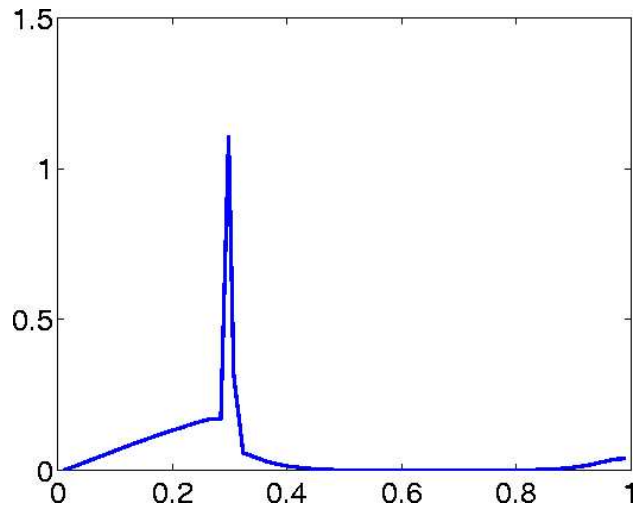
Figure 20: Pointwise error for pressure function along the line y=1/6, div-const method
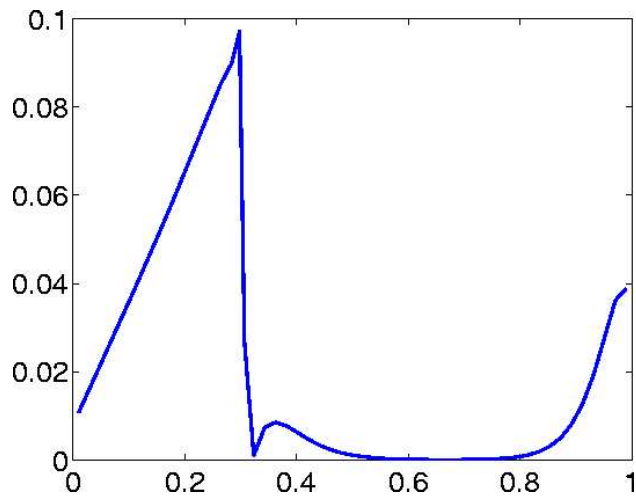
Figure 21: Pointwise error for pressure along the line y=1/6, new method (attention: different scale)
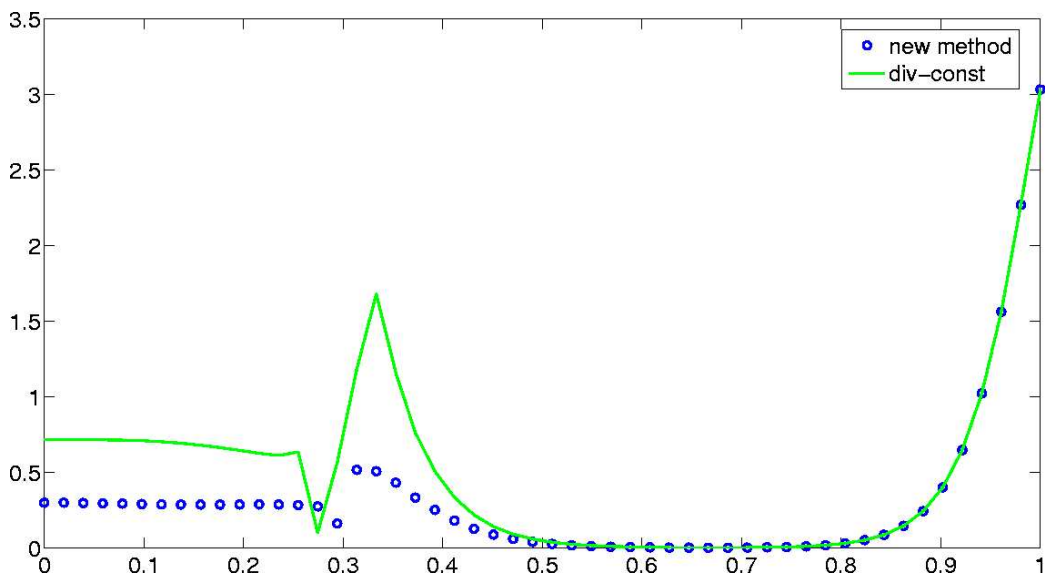
Figure 22: Error for fluxes along the line y=1/6
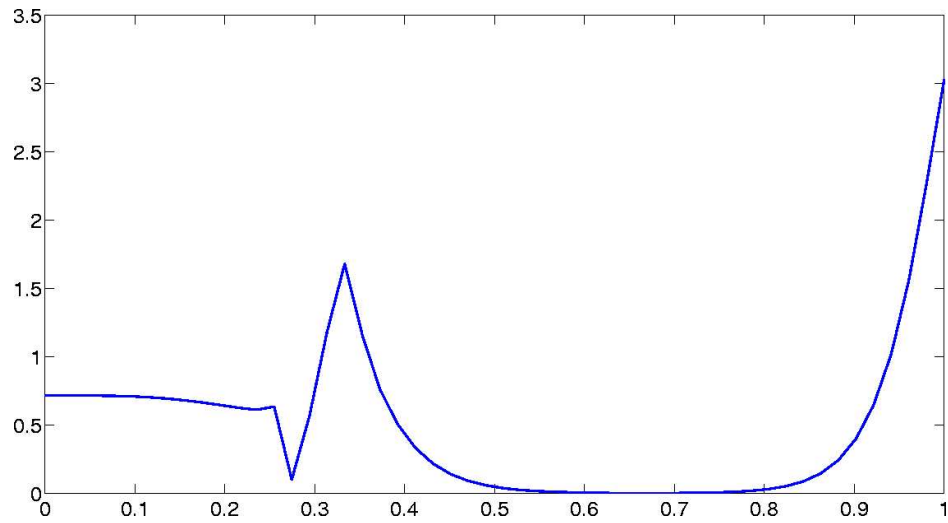
Figure 23: Error for fluxes along the line y=1/6, div-const method
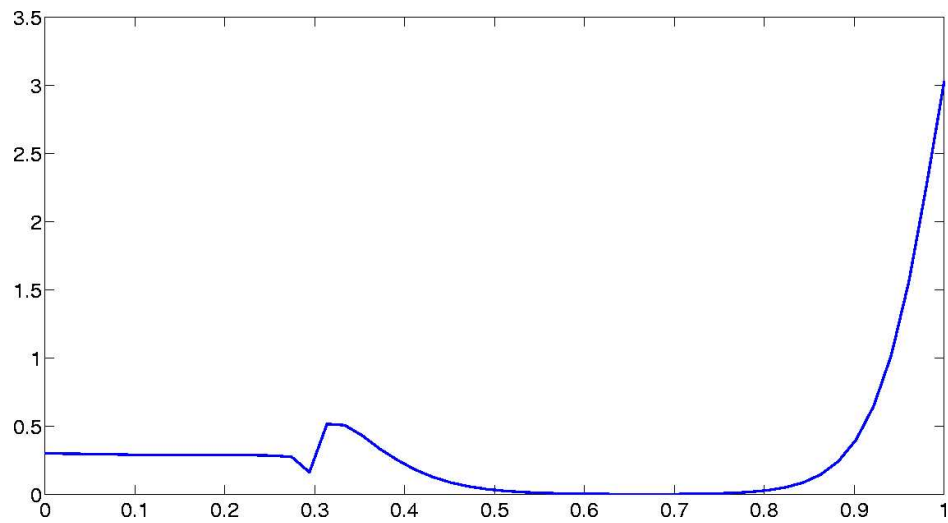
Figure 24: Error for fluxes along the line y=1/6, new method

42

Test Example 3

In the third experiment, we partition Ω into to polyhedrons as shown in Figure 15. The mesh Ω_h is shown in Figure 16.

Input data:

$$a_1 = 500 \qquad a_2 = 1$$

$$c_1 = 1000 \quad c_2 = 0.01$$

$$f_1 = 0.01 \quad f_2 = 1000$$

Boundary conditions:

$$p|_{\Gamma_1} = 0$$

$$p|_{\Gamma_2} = 10$$

$$-(a\nabla p \cdot \mathbf{n})|_{\Gamma_3 \cup \Gamma_4} = 0$$

Mesh step size in $\Omega_h : h = 1/51$.
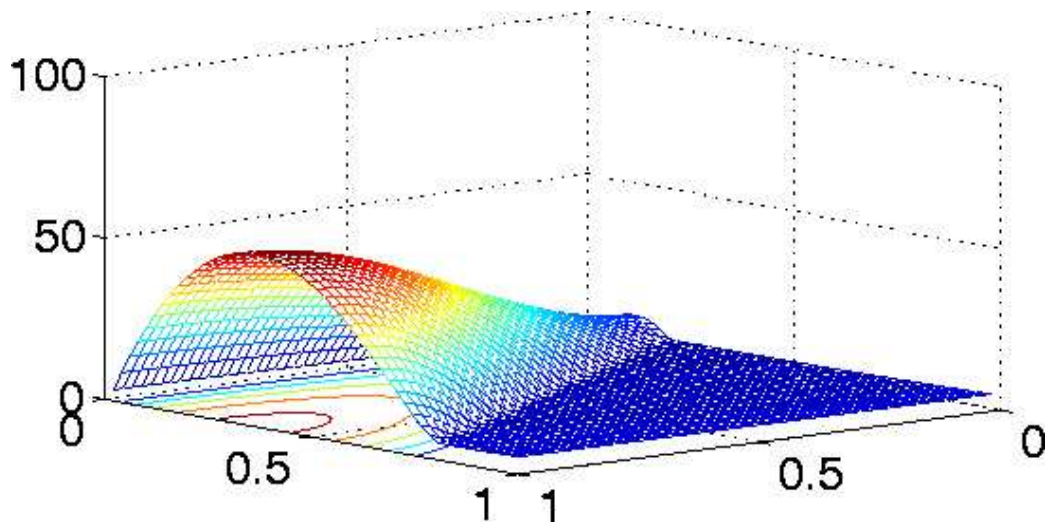
Figure 25: Reference solution
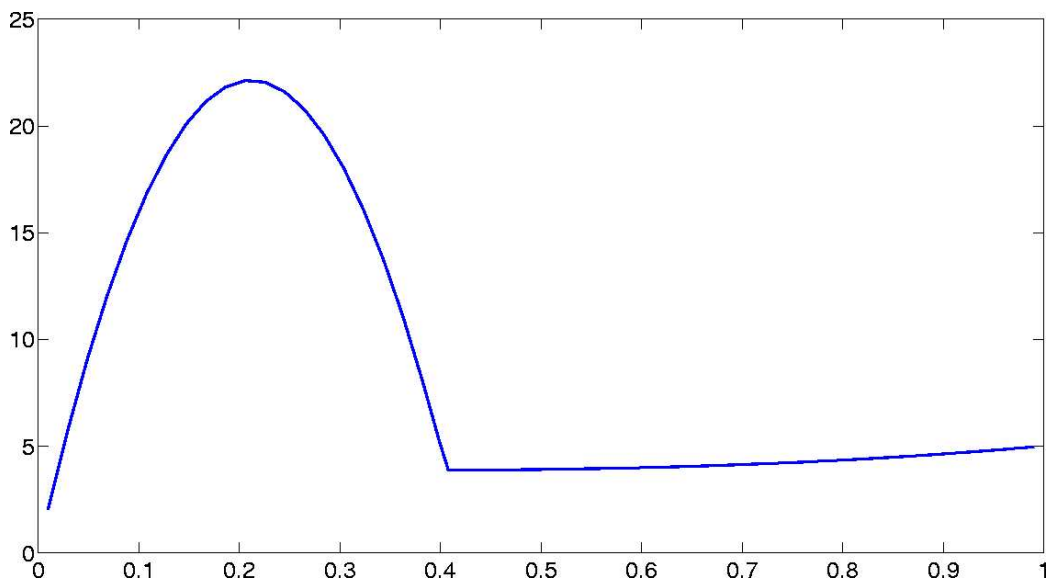
Figure 26: Reference solution along the line y=1/3
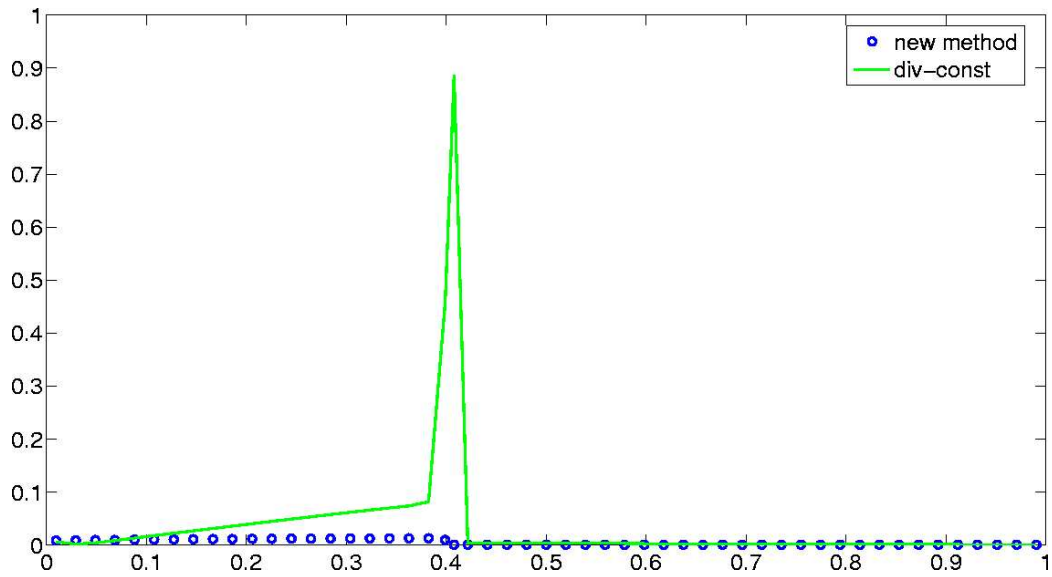
Figure 27: Pointwise error for pressure function along the line y=1/3 (attention: different scale)
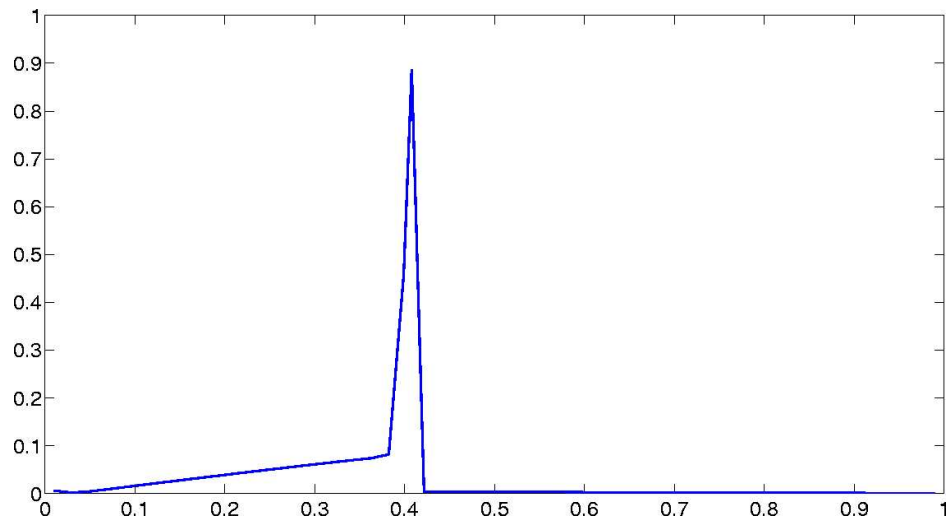
Figure 28: Pointwise error for pressure function along the line y=1/3, div-const method
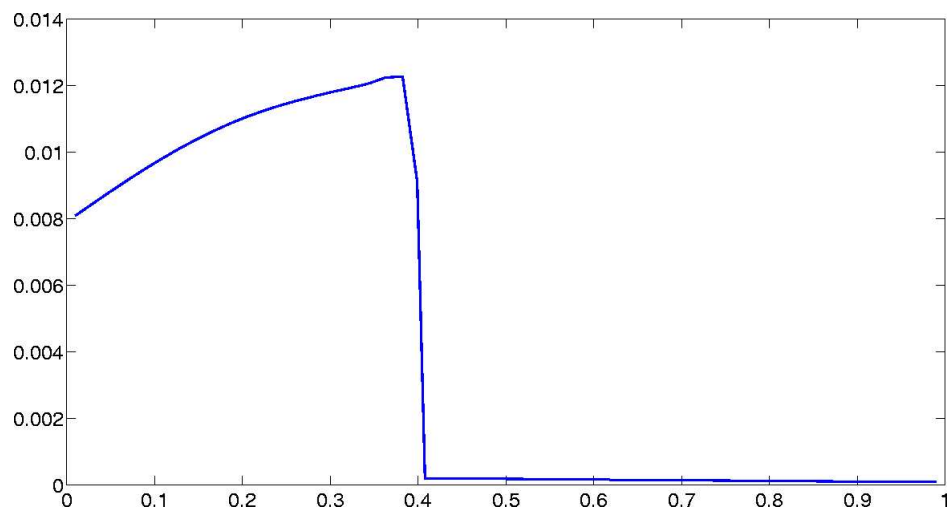
Figure 29: Pointwise error for pressure along the line y=1/3, new method (attention: different scale)
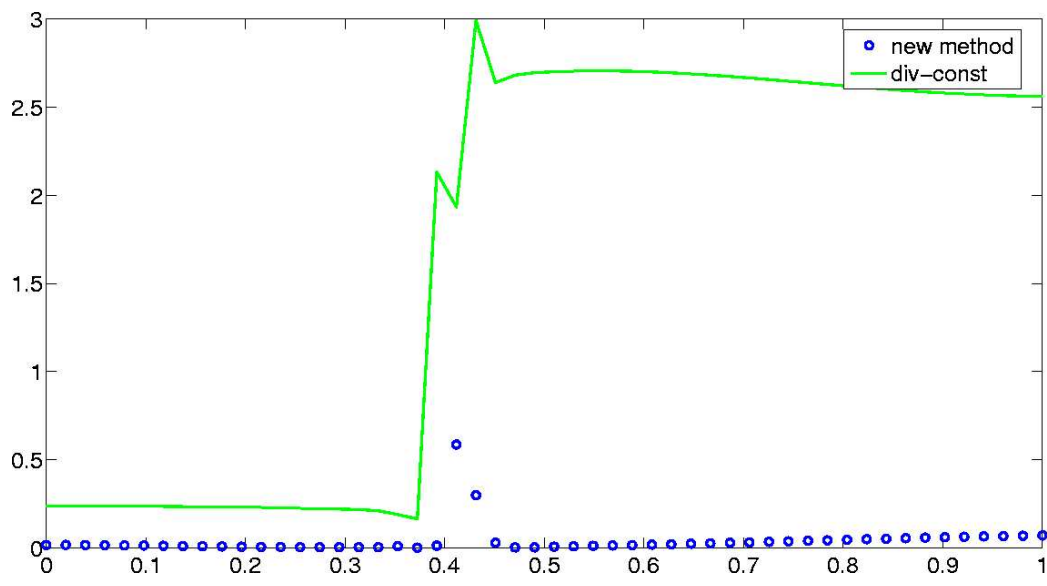
Figure 30: Error for fluxes along the line y=1/3
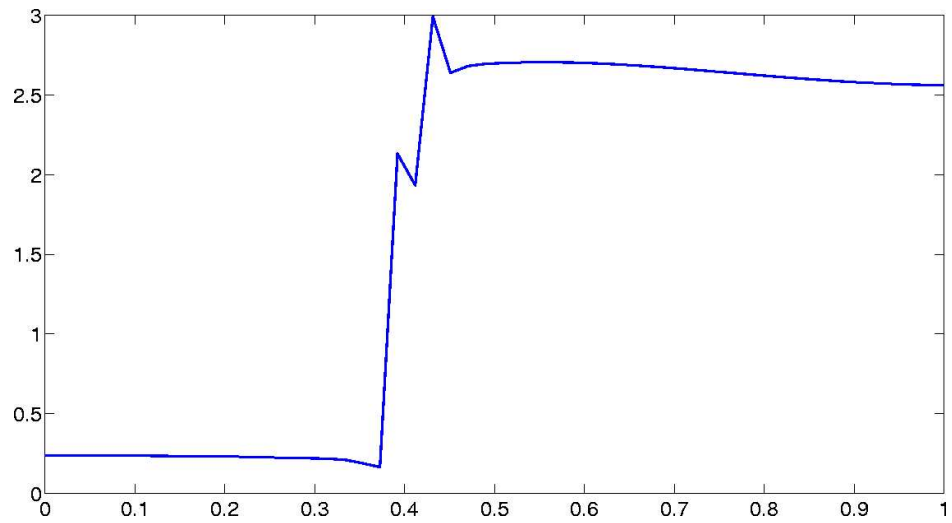
Figure 31: Error for fluxes along the line y=1/3, div-const method
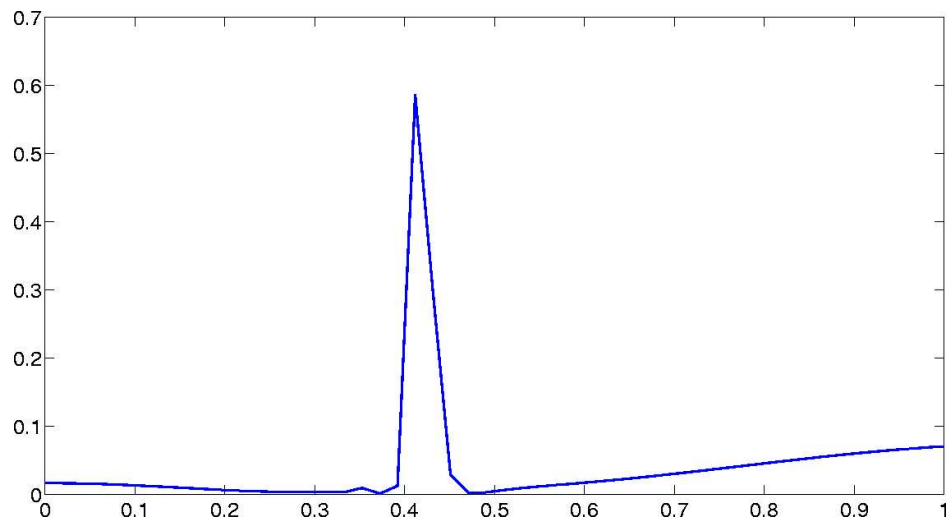
Figure 32: Error for fluxes along the line y=1/3, new method

48

Test Example 4

In the fourth experiment, we partition Ω into four polyhedrons as shown in Figure 33.
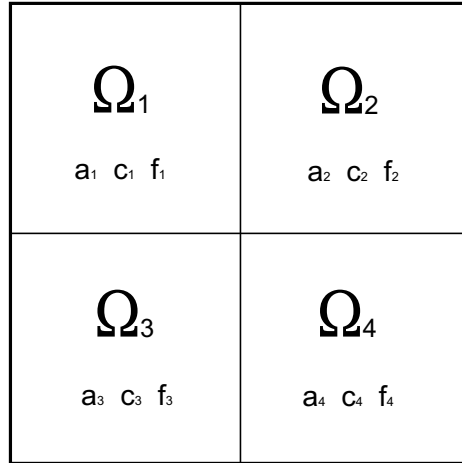
Figure 33: Partitioning of Ω into Ω_1, Ω_2, Ω_3, and Ω_4
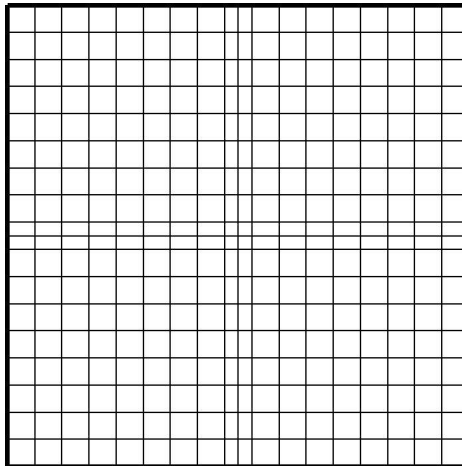
Figure 34: Square mesh Ω_h

Input data:

$$a_1 = 1 \qquad a_2 = 1 \qquad a_3 = 1 \qquad a_4 = 1$$

$$c_1 = 100 \qquad c_2 = 0.001 \quad c_3 = 0.001 \qquad c_4 = 100$$

$$f_1 = 0.001 \qquad f_2 = 100 \qquad f_3 = 100 \qquad f_4 = 0.001$$

Boundary conditions:

$$p|_{\Gamma_1} = 0$$

$$p|_{\Gamma_2} = 10$$

$$-(a\nabla p \cdot \mathbf{n})|_{\Gamma_3 \cup \Gamma_4} = 0$$

Mesh step size in Ω_h: $h = 1/51$
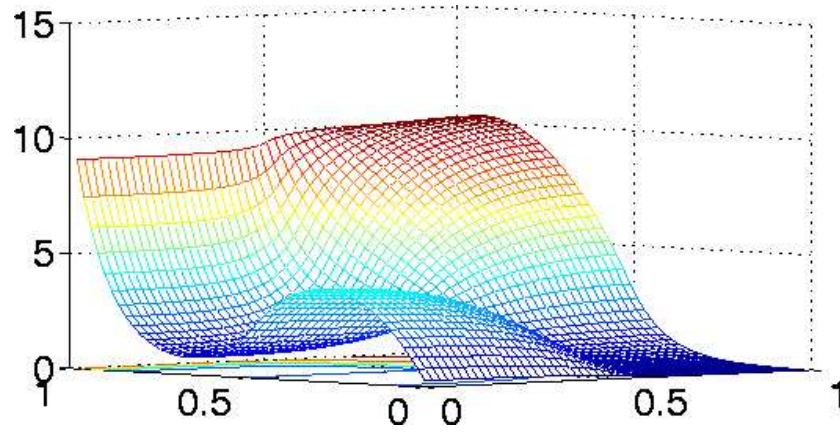
Figure 35: Reference solution
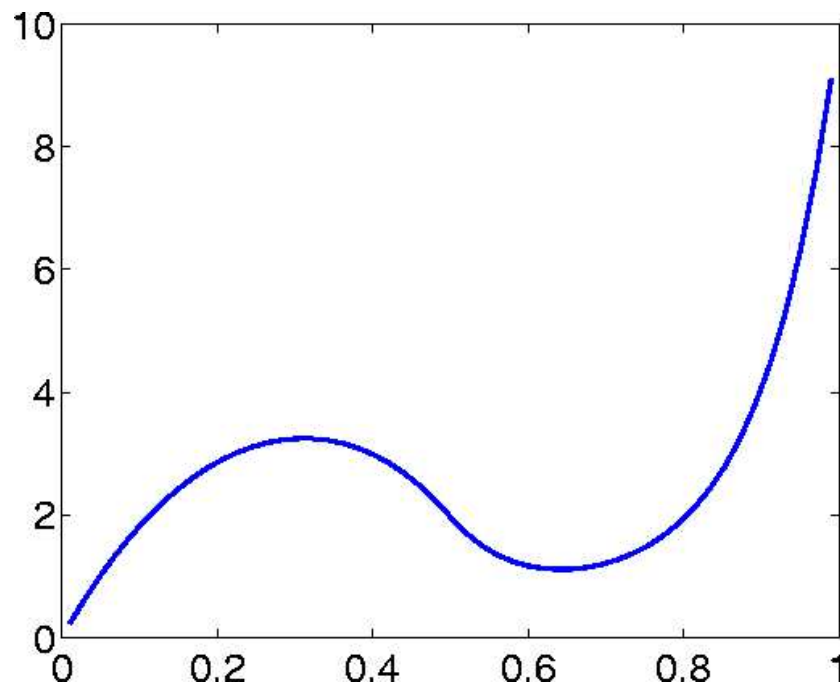
Figure 36: Reference solution along the line y=1/3
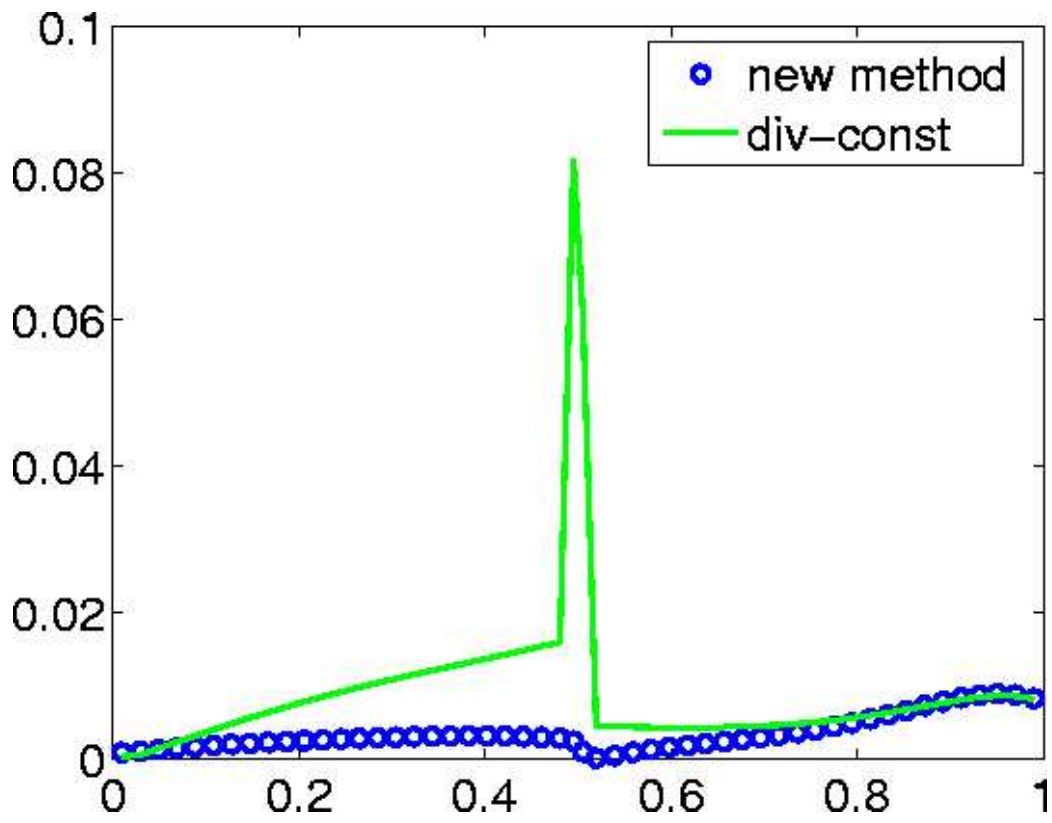
Figure 37: Pointwise error for pressure function along the line y=1/3
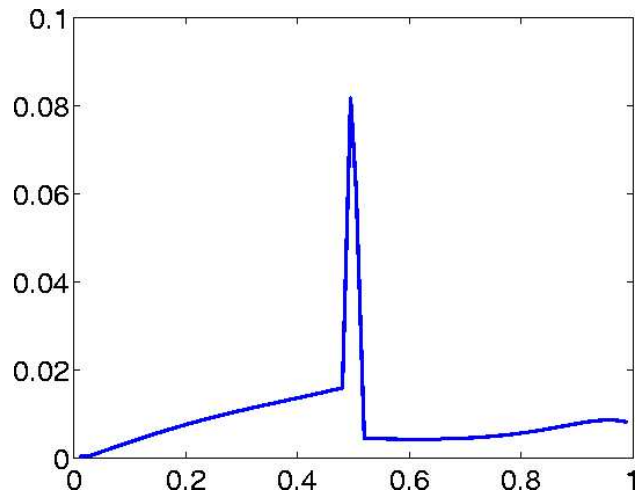
Figure 38: Pointwise error for pressure function along the line y=1/3, div-const method
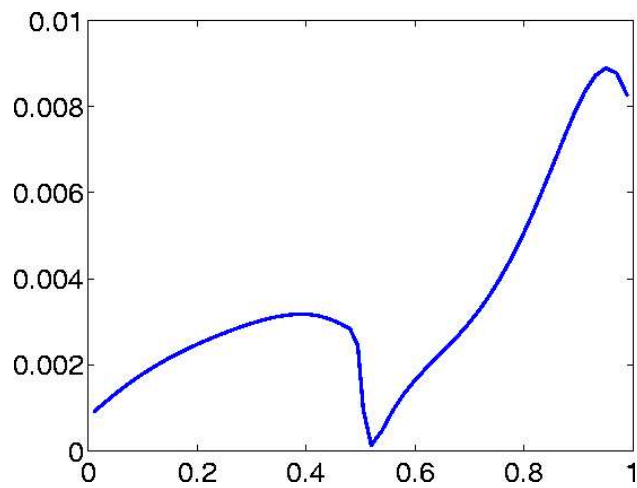
Figure 39: Pointwise error for pressure function along the line y=1/3, new method (attention: different scale)
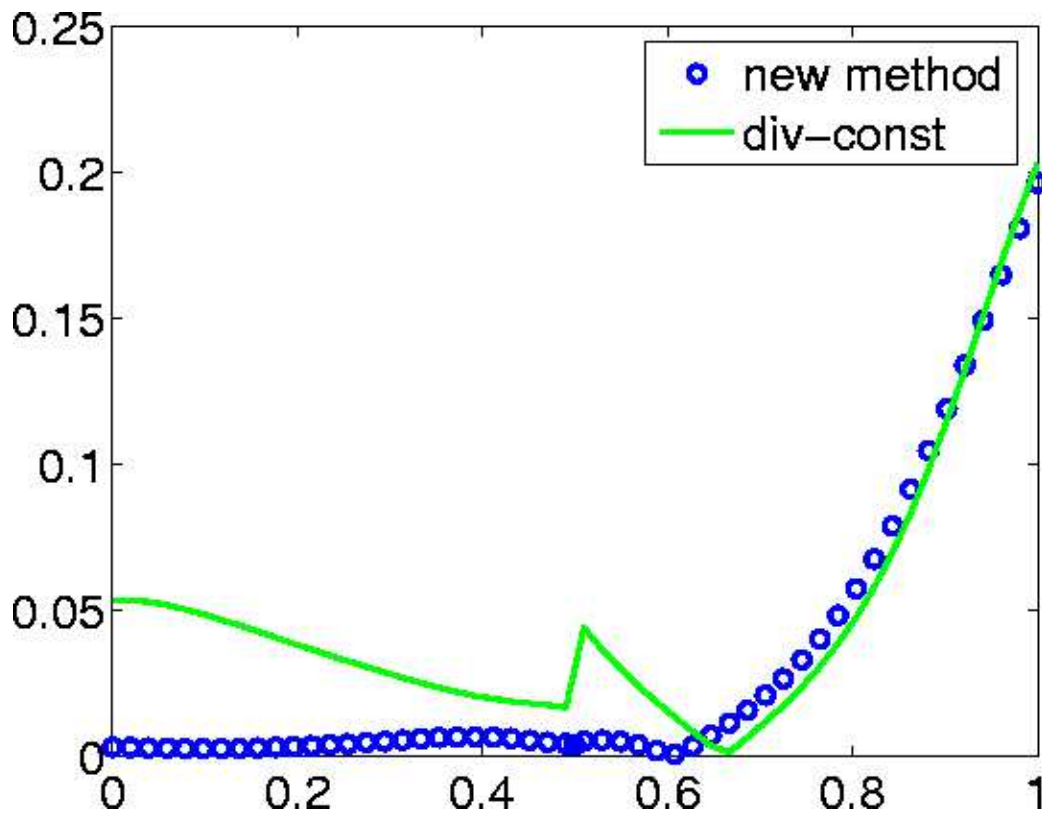
Figure 40: Error for fluxes along the line y=1/3
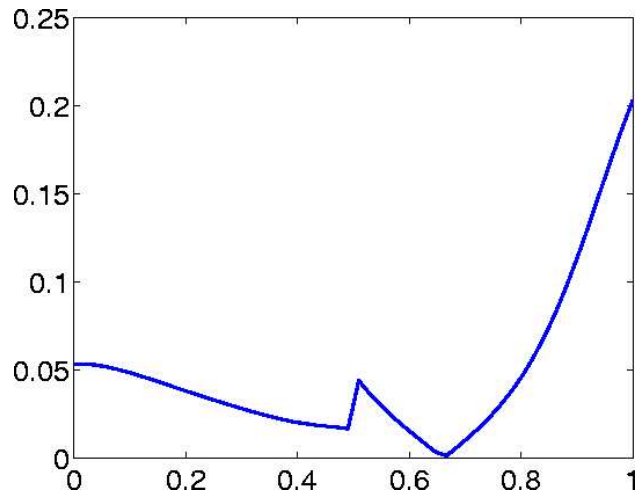
Figure 41: Error for fluxes along the line y=1/3, div-const method
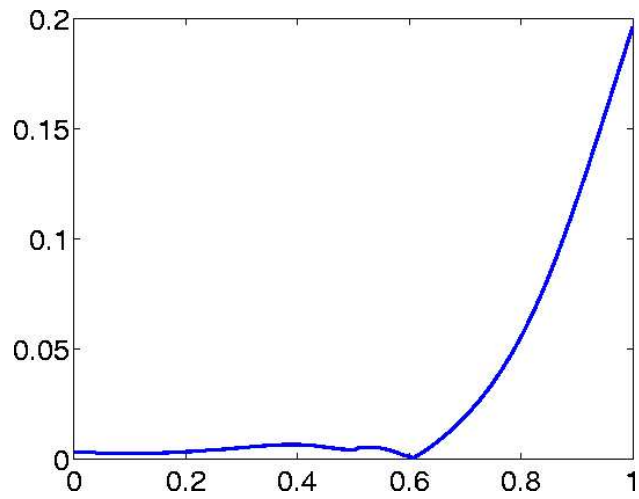
Figure 42: Error for fluxes along the line y=1/3, new method

55

Test Example 5

In the fifth experiment, we partition Ω into four polyhedrons as shown in Figure 33.

Input data:

$$a_1 = 1 \qquad a_2 = 500 \qquad a_3 = 800 \qquad a_4 = 2$$

$$c_1 = 100 \qquad c_2 = 0.001 \qquad c_3 = 0.001 \qquad c_4 = 100$$

$$f_1 = 0.001 \qquad f_2 = 100 \qquad f_3 = 100 \qquad f_4 = 0.001$$

Boundary conditions:

$$p|_{\Gamma_1} = 0$$

$$p|_{\Gamma_2} = 10$$

$$-(a\nabla p \cdot \mathbf{n})|_{\Gamma_3 \cup \Gamma_4} = 0$$
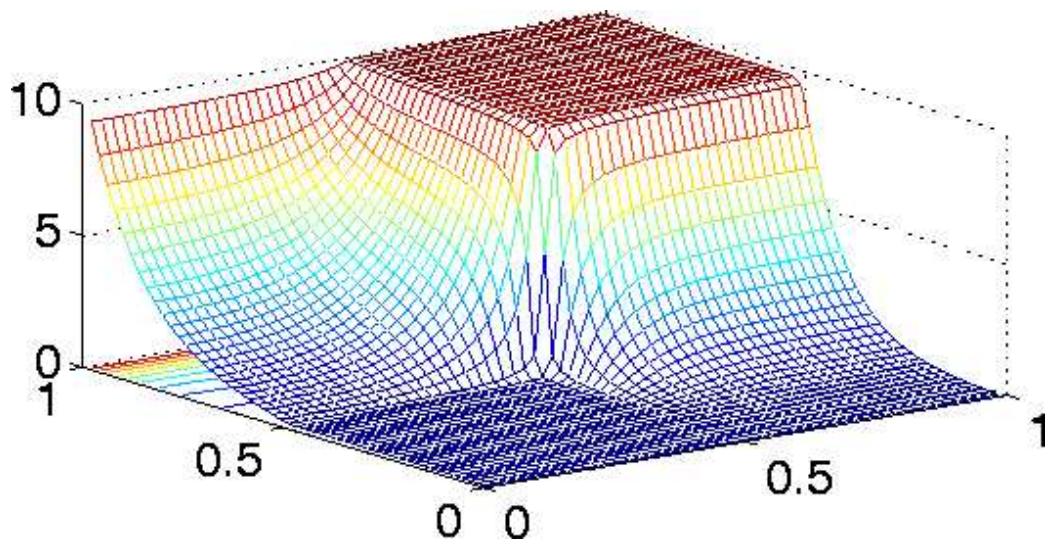
Figure 43: Reference solution
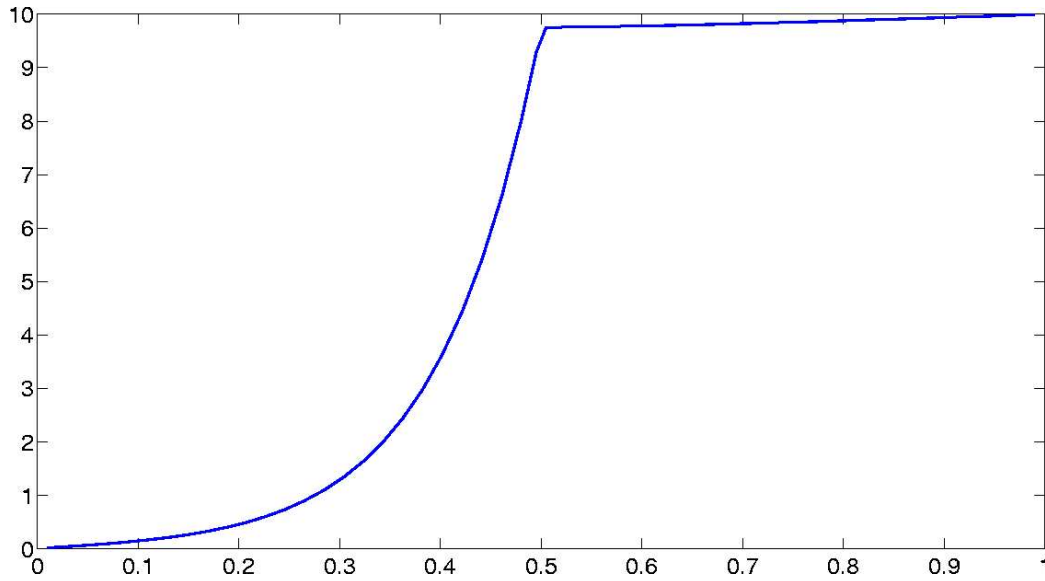
Figure 44: Reference solution along the line y=1/3
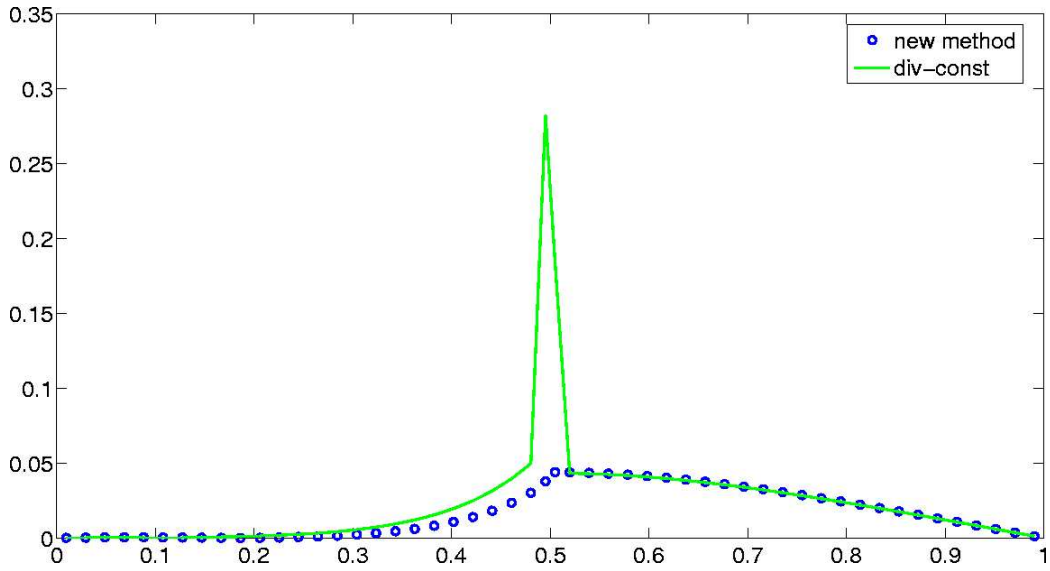
Figure 45: Pointwise error for pressure function along the line y=1/3
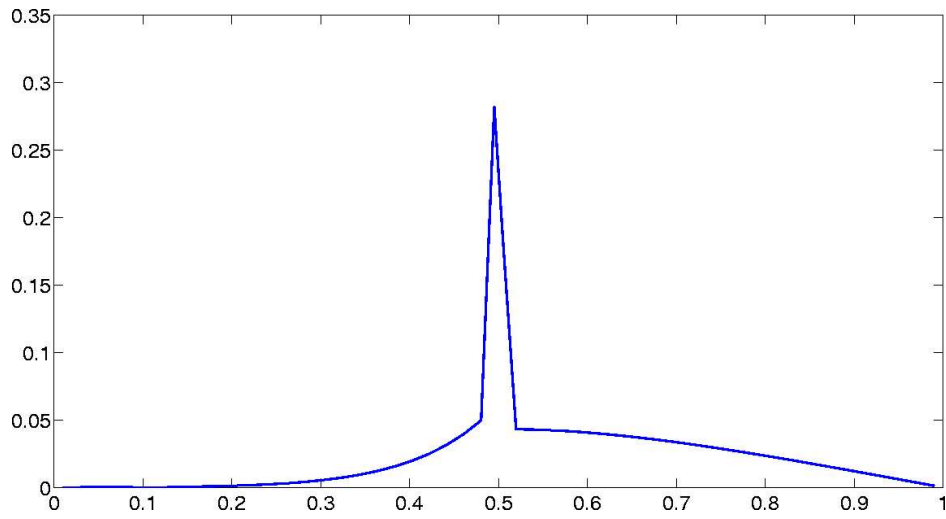
Figure 46: Pointwise error for pressure function along the line y=1/3, div-const method
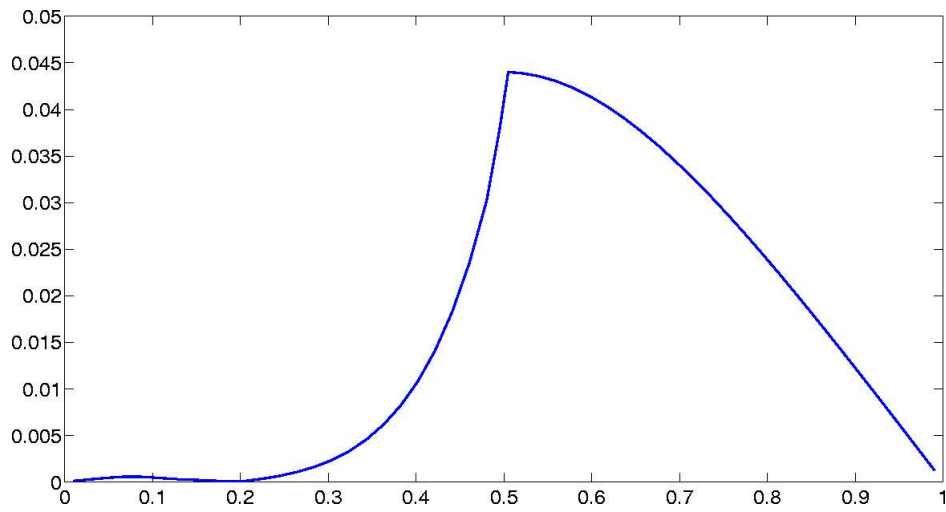
Figure 47: Pointwise error for pressure function along the line y=1/3, new method (attention: different scale)

59

6 Generalizations

1. The extension to 3D problems can be done just by replacing in Section 3 the word "polygon" by the word "polyhedron". Of course, the description of the method for 3D problems is more complicated technically.

2. The multilevel extension of the method is also obvious. On the first level we have to partition polygonal cells $E_k^{(0)} \equiv E_k$ into smaller polygons $\{E_{k,l}^{(1)}\}$ and to assume that the discretization scheme on the smaller polygonal cells is known. Then, the procedure can be repeated until we get the triangular partitionings.

7 Acknowledgments

References

[1] F. Brezzi and M. Fortin, *Mixed and hybrid finite element methods.* Springer Verlag, Berlin, 1991

[2] J. Hyman, M. Shashkov, and S. Steinberg, The numerical solution of diffusion problems in strongly heterogeneous non-isotropic materials, *J. Comput. Phys.*, (1997), **132**, pp. 130–148

[3] Yu. Kuznetsov and S. Repin, New mixed finite element method on polygonal and polyhedral meshes, *Russian J. Numer. Anal. Math. Modelling*, (2003), **18**, pp. 261–278

[4] Yu. Kuznetsov, K. Lipnikov, and M. Shashkov, The mimetic finite difference method on polygonal meshes for diffusion-type problems, *Computational Geosciences*, (2004), **8**, pp. 301–324